Inelastic X-ray Scattering by Electronic Excitations

The Taiwan Beamline Perspective (BL12XU@SPring-8)

Yong Cai
SPring-8 Group
National Synchrotron Radiation Research Center, Taiwan

NSLS-II Seminar, 11 April 2007

The Taiwan Beamlines at SPring-8

- **The biggest scientific investment overseas for Taiwan in her history**
  - **US$10M initial construction cost for 5 years, subsequent annual operation and instrumentation upgrade budget US$500 ~ 800K (excl. salary)**
- **Motivation: To extend Taiwan Light Source's spectral range to hard x-rays**

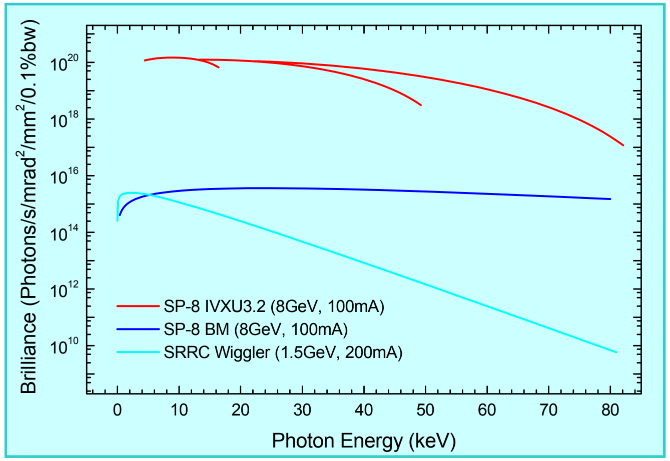

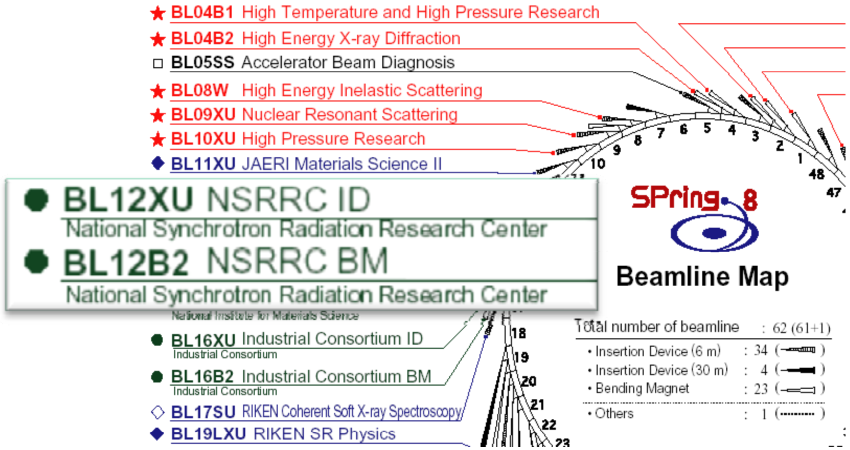

- **Two Beamlines:**
  - **BL12B2: Biostructure & Materials Research**

    Multiple Purposes (Scattering, Powder Diffraction, Protein Crystallography)
  - **BL12XU: Inelastic X-ray Scattering**

    For a broad range of applications, focusing on the study of electronic excitations in correlated electron systems and high-pressure physics (sciences)

Location and Access

- **Close Proximity:**
  - Flight time 2.5 hours between Taipei and Osaka (Kansai Airport)
  - Fast train connection 2.5 hours from Kansai to SPring-8
  - Almost the same time zone

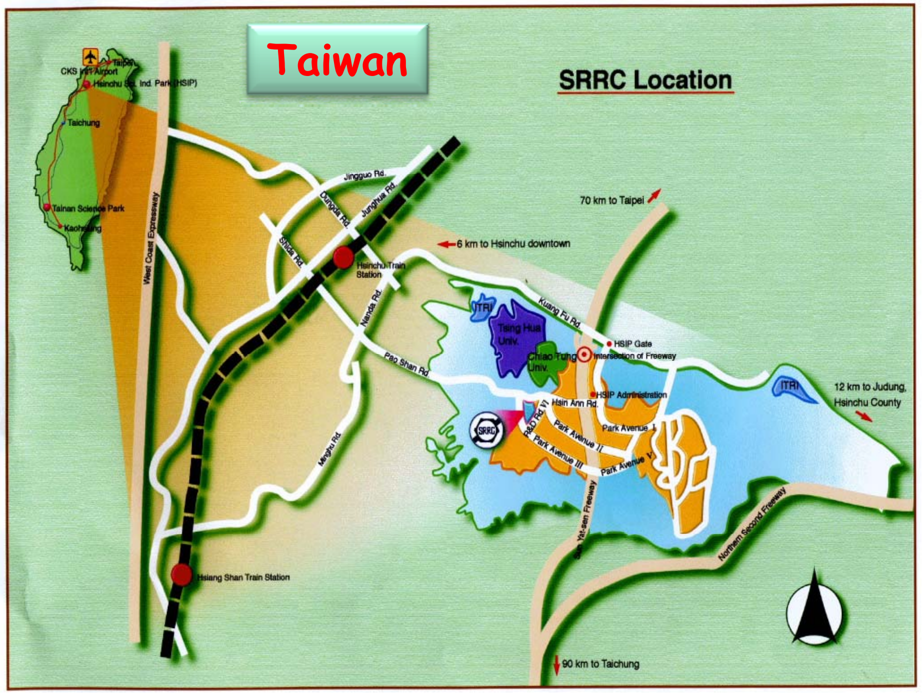

SPring-8 Site

Outline

- Brief Review of IXS by Electronic Excitations
  - Theory and Experiment (BL12XU Setup)
- Performance and Selected Results
  - Element-Specific Applications (XRS/XES/FPY-XAS)

    XRS: High pressure phases of H_2O, liquid & solid He, SiO_2, Ba_8Si_{46} ...

    XES/XAS: P/T-induced charge instability in TmTe, Prussian Blue ...
  - Low-Energy Charge Dynamics in (ω,q) Space (NIXS/RIXS)

    NIXS: Graphite, MgB_2, Py-SO, $CaMnO_3$, NiO ...

    RIXS at the K-edge of TM: NiO, Sr_2CuO_3, La_2CuO_4/La_2NiO_4 ...
- Possible Further Developments and Outlook
  - Possible further developments
  - Outlook with the Taiwan Photon Source

IXS by Electronic Excitations

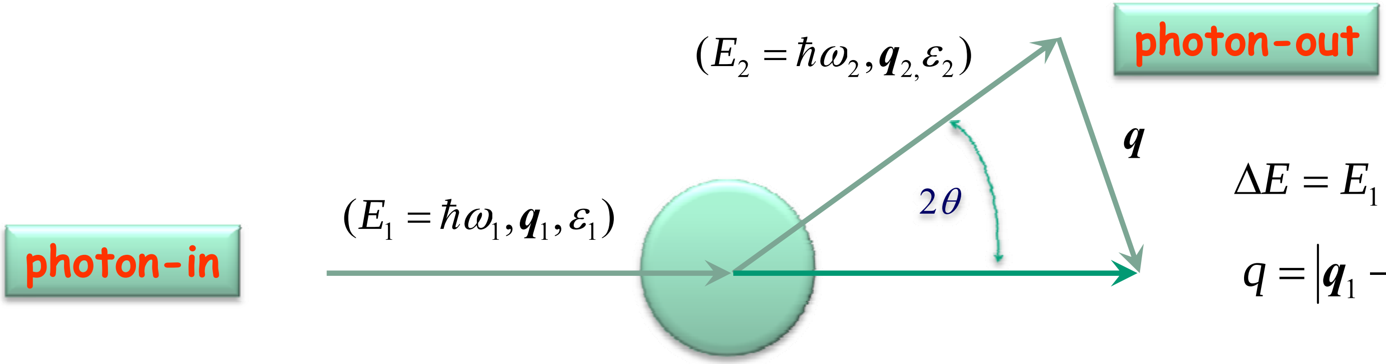

$$\Delta E = E_1 - E_2 = \hbar\omega$$

$$q = |\boldsymbol{q}_1 - \boldsymbol{q}_2| = 2q_1 \sin(2\theta/2)$$

A rather weak scattering probe:

$$\left(\frac{d\sigma}{d\Omega}\right)_0 = r_0^2 \left(\vec{e}_i \cdot \vec{e}_f\right)^2 \left(\frac{\omega_f}{\omega_i}\right) \approx 10^{-25}\,\mathrm{cm}^2$$

Hard x-rays:
Thomson scattering

$$\left(\frac{d\sigma}{d\Omega}\right)_0 = \frac{4}{a_B{}^2 q^4} \approx 10^{-15}\,\mathrm{cm}^2$$

Fast electrons:
Rutherford scattering

Therefore IXS measures properties of the scattering system by itself, but requires intense hard x-ray beam for practical applications

⟹ **Possible only with 3rd generation photon sources !!**

National Synchrotron Radiation Research Center

SPring-8

(Yong Cai, NSLS-II Seminar, 11 April 2007)

Advantages of IXS

… as compared to other scattering probes (light, neutrons, electrons)

- **Kinematics**
  - Accessible (ΔE, q) covers the full range of dielectric response: ΔE : meV ~ keV q : typical BZ sizes
  - ΔE and q are effectively decoupled

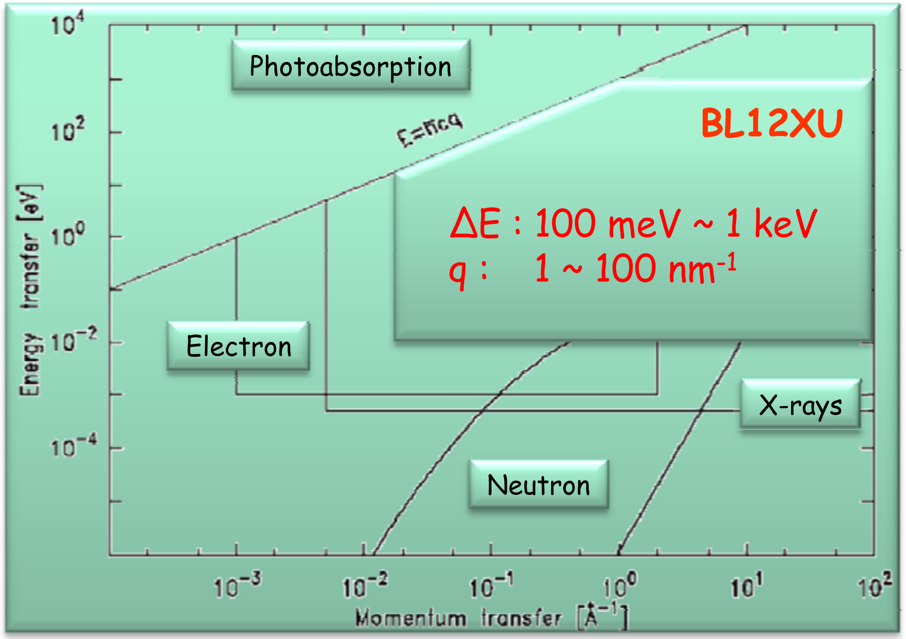

- **Coupling to matter**
  - Coupled directly to the electronic charge, therefore sensitive to all kinds of electronic excitations
  - Truly bulk-sensitive, in comparison with VUV and SX photoemission and absorption
  - Applicable to systems under external environments (high pressure, electric and magnetic fields, high and low temperatures, etc.), and systems that are not compatible with vacuum (e.g., liquids)
  - Energy tuneability provides element specific experiments (XRS/XES/PFY-XAS)
  - Small beam size offers the possibility to study small samples (incl., HP-DAC samples)

Resonant and/or Non-resonant IXS?

- **Interaction Hamiltonian with Electrons**

  (neglecting spin and orbital degrees of freedom)

$$H_{int} = H_{int}^{(1)} + H_{int}^{(2)} = \sum_j \frac{e^2}{2mc^2}\mathbf{A}_j^2 + \sum_j \frac{e}{mc}\mathbf{A}_j \cdot \mathbf{p}_j$$

- $\mathbf{A}^2 - term$: 1st order expansion, photon-in photon-out process
- $\mathbf{A}\cdot\mathbf{p} - term$: 2nd order expansion, involving intermediate states

- **Double Differential Cross Section**

$$\frac{d^2\sigma}{d\Omega d\omega_2} \propto \sum_{I,F} \left| \left\langle F \left| H_{int}^{(1)} \right| I \right\rangle + \sum_N \frac{\left\langle F \left| H_{int}^{(2)} \right| N \right\rangle \left\langle N \left| H_{int}^{(2)} \right| I \right\rangle}{E_N - (E_I + \hbar\omega_1) - i\Gamma_N} + \ldots \right|^2$$

Non-resonant | Resonant

Non-resonant IXS (NIXS):

$$\frac{d^2\sigma}{d\Omega d\omega_2} = \left(\frac{d\sigma}{d\Omega}\right)_0 S(\mathbf{q},\omega)$$

$$S(\mathbf{q},\omega) = -\frac{\hbar q^2}{4\pi^2 e^2 n}\cdot \mathrm{Im}\,\varepsilon^{-1}(\mathbf{q},\omega) = -\frac{1}{\pi n}\cdot \mathrm{Im}\,\chi(\mathbf{q},\omega)$$

- $S(q,\omega)$: charge density-density correlation function
- Fluctuation-dissipation theorem provides the macroscopic connection
- First-principles calculations possible

Resonant IXS (RIXS):

- Secondary processes involving intermediate states
- Resonant enhancement
- Element, charge, and spin specific experiments (RXES/PFY-XAS)
- Non-dipole excitations
- Theo: Model dependent

IXS Spectroscopic Information

- **NIXS (XRS/XES/PFY-XAS)**

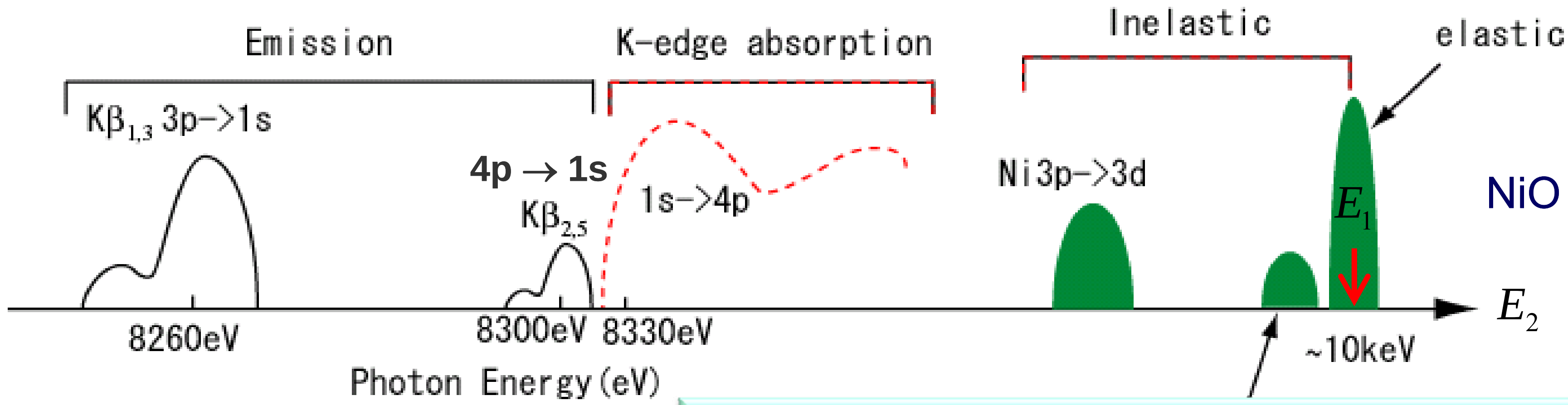

Loss features by phonons, magnons, orbitons, excitons, gap excitations, plasmons, and electron-hole pair excitations, etc

- **RIXS (RXES/PFY-XAS)**

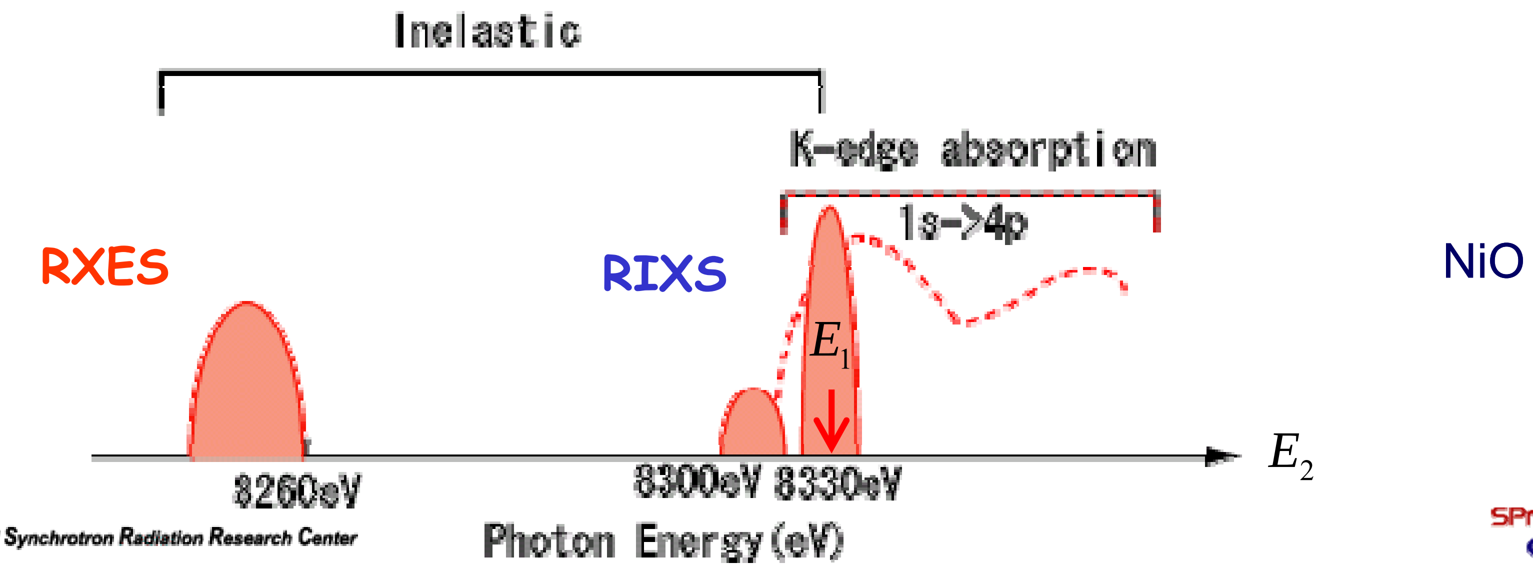

National Synchrotron Radiation Research Center

SPring-8

(Yong Cai, NSLS-II Seminar, 11 April 2007)

Taiwan IXS Beamline (BL12XU@SPring-8)

- **Design principle 1: Maximize the flux within the required energy width !**

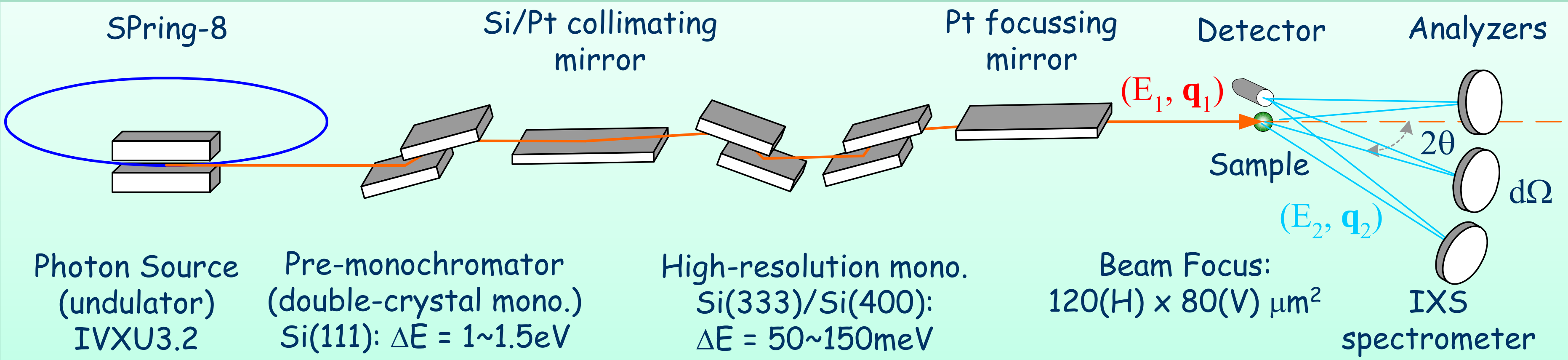

- **Design principle 2: Maximize flexibility to accommodate changing needs !**

- Total energy resolution : 60 ~ 350 meV, or ~ 1 eV with DCM beam
- Flux: 1 x 10^{13} photons/sec/eV, and basically scaled with band width
- Beam size : 120 x 80 μm^2 (16 x 20 μm^2 optional with KB mirrors)
- Energy transfer range: 100 meV ~ 1 keV with a single setup
- q-range : 1 ~ 100 nm^{-1}
- Count-rate : 0.1 ~ 100 cps (system dependent)

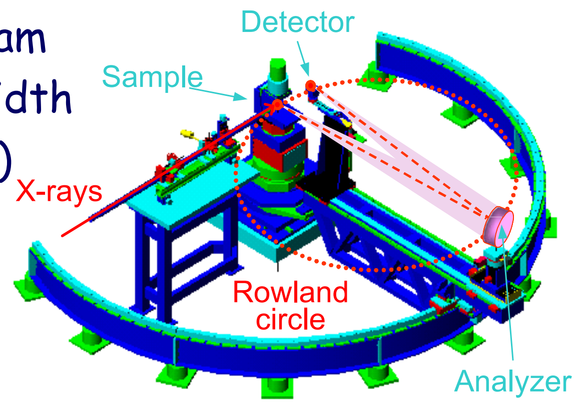

National Synchrotron Radiation Research Center

(Cai et al, AIP Conf. Proc. 705, 340)

(Yong Cai, NSLS-II Seminar, 11 April 2007)

Taiwan IXS Beamline (BL12XU@SPring-8)

- **Micro focusing system (optional), compact and low cost**

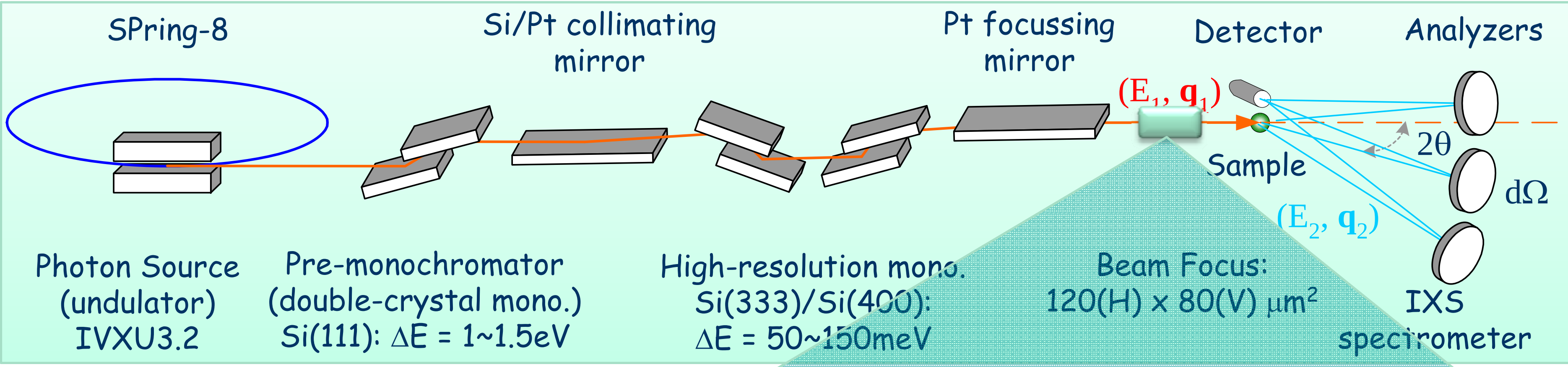

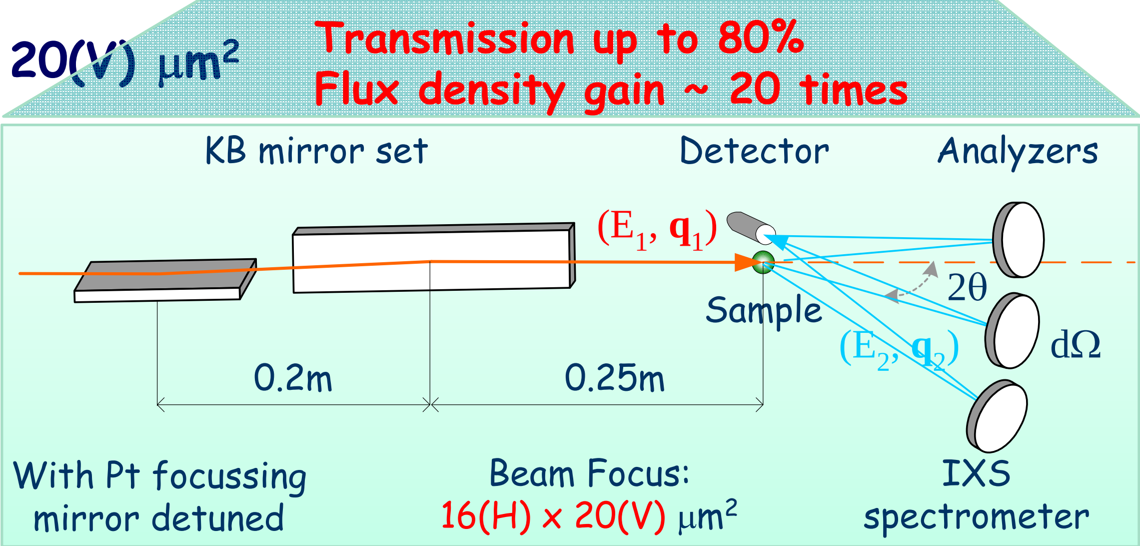

- **Routinely achieving 16(H) x 20(V) μm^2**

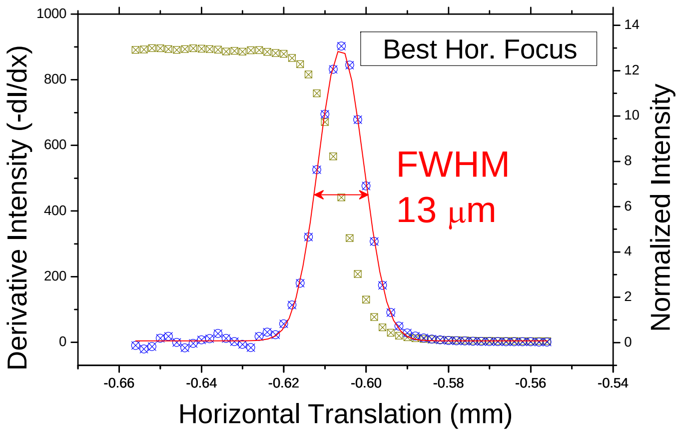

National Synchrotron Radiation Research Center

(Huang et al, AIP Conf. Proc. 879, 971)

SPring-8

(Yong Cai, NSLS-II Seminar, 11 April 2007)

Spectrometer Setups

- NIXS Setup
- RIXS Setup

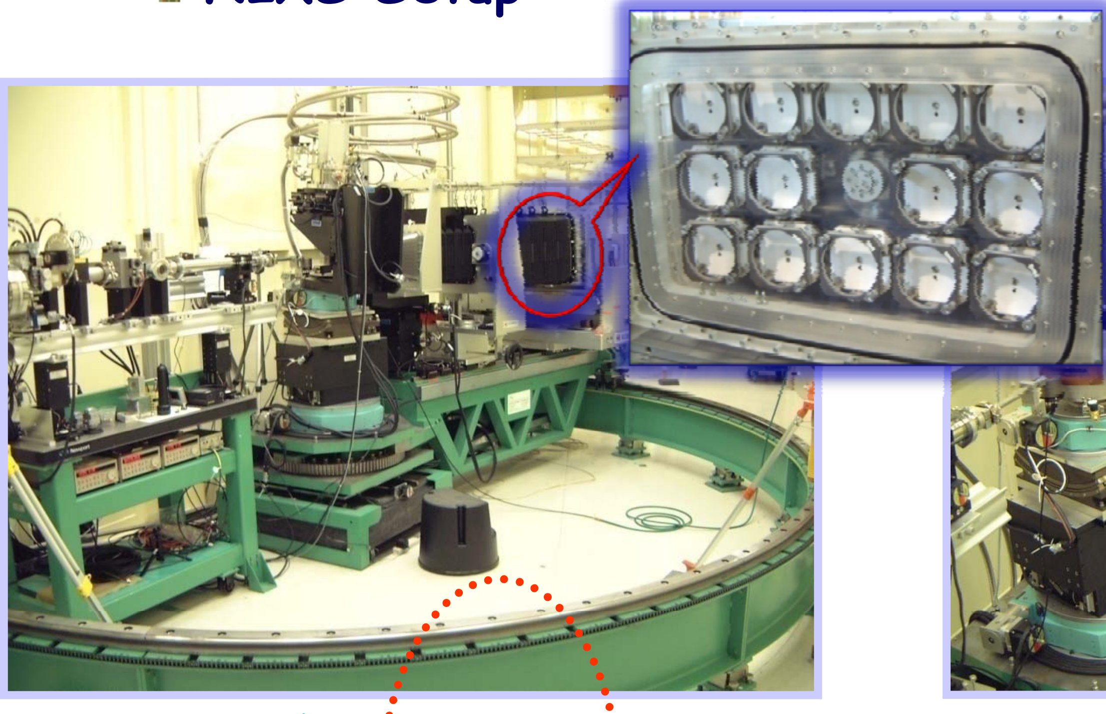

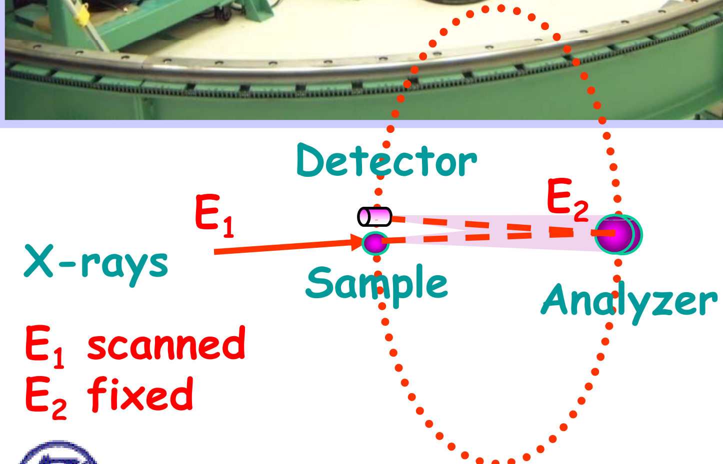

E_1 scanned
E_2 fixed

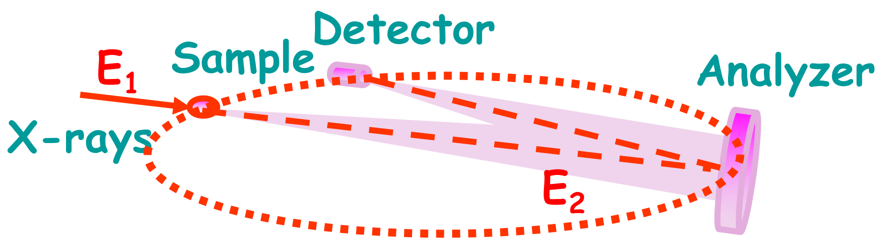

E_1 fixed but stepped thru edge, E_2 scanned
CFS: E_1 & E_2 scanned together

National Synchrotron Radiation Research Center

(Yong Cai, NSLS-II Seminar, 11 April 2007)

X-ray Crystal Analyzers

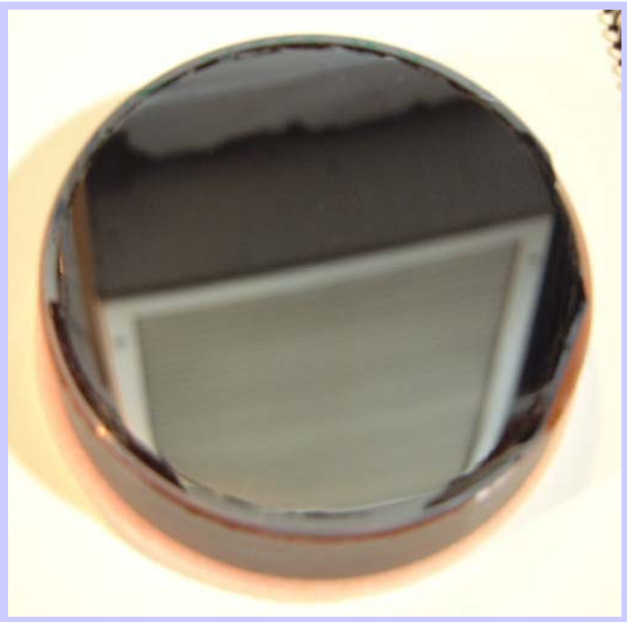

Spherically bent Si(111) analyzer

- Bending radius: 2m
- Diameter: 100mm
- Wafer thickness: 0.5mm
  diced with the DRIE technique.

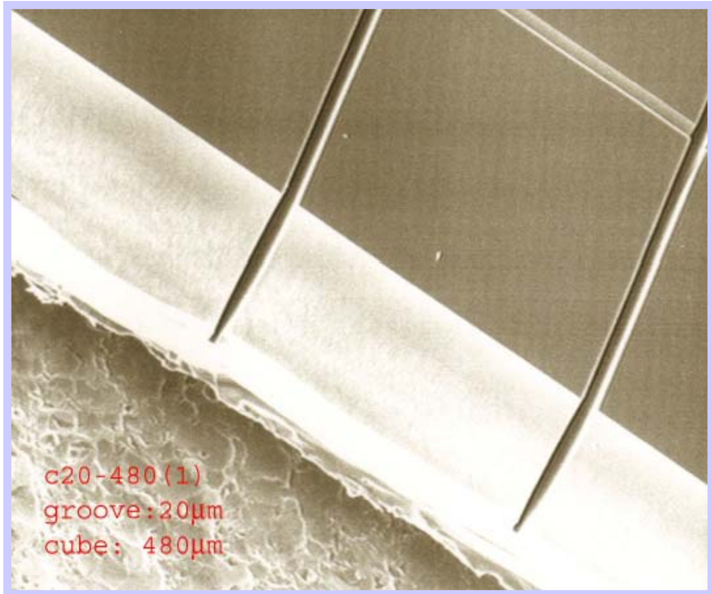

SEM image of a Si(111) test wafer diced with the DRIE technique under similar conditions as those for the analyzer shown on the left.

(Shew et al, SPIE Proc. 4783, 131)

Analyzer Performance

Bent Analyzer

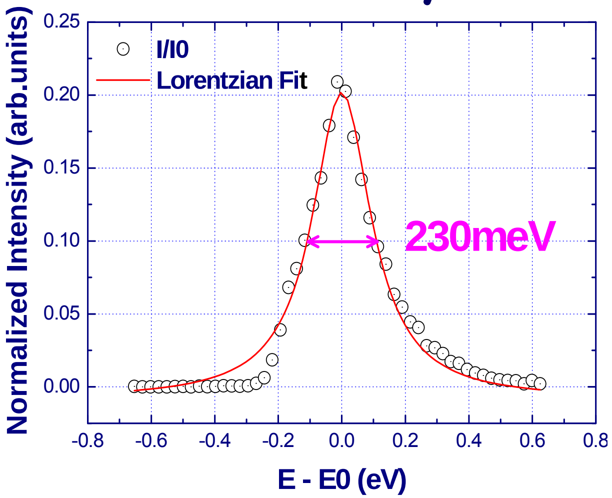

DRIE Analyzer

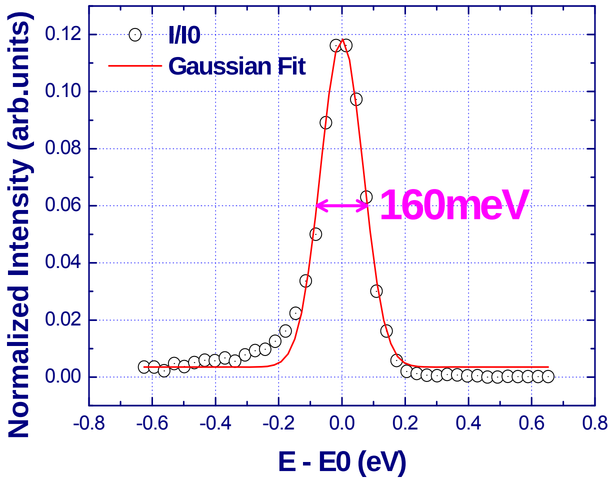

Diced Analyzer

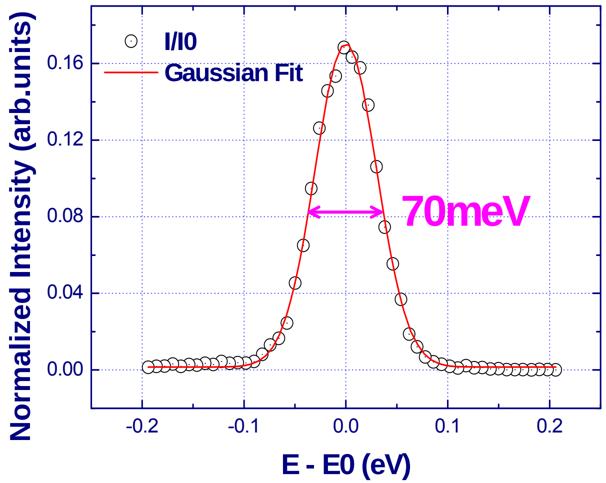

Test Conditions

- Incident Beam: 50 meV width @ 9886.2 eV
- Scatter: 2 mm thick PMMA
- Analyzer: 2-m bending radius, Si(555) reflection at near backscattering

⇨ Controlled dicing tailors the strain left in the wafer, allowing tuning of the energy resolution to match the incident beam band width
- The most efficient configuration for a given energy resolution !

RIXS Analyzers (R=1,2m)

		θ=89deg	3d Transitional Metal K-edge									θ=60deg
Si (hkl)	**Back Scattering**	**Emin**	**Ti**	**V**	**Cr**	**Mn**	**Fe**	**Co**	**Ni**	**Cu**	**Zn**	**Emax**
004	4.5661	4.5918	Ti									5.2725
133	4.9758	5.0038		V								5.7455
224	5.5923	5.6237			Cr							6.4574
115	5.9315	5.9649				Mn						6.8491
333	5.9315	5.9649										6.8491
044	6.4574	6.4937					Fe					7.4564
135	6.7533	6.7913						Co				7.7981
026	7.2196	7.2602							Ni			8.3365
335	7.4855	7.5276										8.6435
444	7.9087	7.9532								Cu		9.1322
117	8.1521	8.1979										9.4132
155	8.1521	8.1979										9.4132
246	8.5424	8.5904									Zn	9.8639
137	8.7682	8.8175										10.1247
355	8.7682	8.8175										10.1247
008	9.1322	9.1835										10.5449
337	9.3438	9.3963										10.7893

National Synchrotron Radiation Research Center

Available analyzers

SPring-8

(Yong Cai, NSLS-II Seminar, 11 April 2007)

Configurations and Performance

NIXS Setups

Beamline @ 9884.7 eV			IXS Spectrometer	
HRM Configuration	Flux ($\times 10^{11}$ photons/sec)	Bandwidth (meV)	Multiple Analyzer(s)	Resolution (meV)
Si(333)	1.5	50	Si(555) 2m diced (x9)	70
Si(400)	5.7	150	Si(555) 2m diced (x9)	175
			Si(555) 2m bent (x3)	300
None (DCM)	120	1250	Si(555) 1m bent (x1)	1300

RIXS Setups

Beamline		IXS Spectrometer		
Resolution Mode	Bandwidth ($\Delta E/E$)	Spherical Analyzer	Energy Range (eV)	Resolution (eV)
LR: Si(111) DCM	1.4×10^{-4}	1m bent	Various edges	~1
HR: Si(400) HRM	1.5×10^{-5}	2m bent	Various edges	~0.35

Outline

- Brief Review of IXS by Electronic Excitations
  - Theory and Experiment (BL12XU Setup)
- **Performance and Selected Results**
  - **Element-Specific Applications (XRS/XES/FPY-XAS)**

    XRS: High pressure phases of H_2O, liquid & solid He, SiO_2, Ba_8Si_{46} ...

    XES/XAS: P/T-induced charge instability in TmTe, Prussian Blue ...
  - Low-Energy Charge Dynamics in (ω,q) Space (NIXS/RIXS)

    NIXS: Graphite, MgB_2, Py-SO, $CaMnO_3$, NiO ...

    RIXS at the K-edge of TM: NiO, Sr_2CuO_3, La_2CuO_4/La_2NiO_4 ...
- Possible Further Developments and Outlook
  - Possible further developments
  - Outlook with the Taiwan Photon Source

Why Study H_2O?

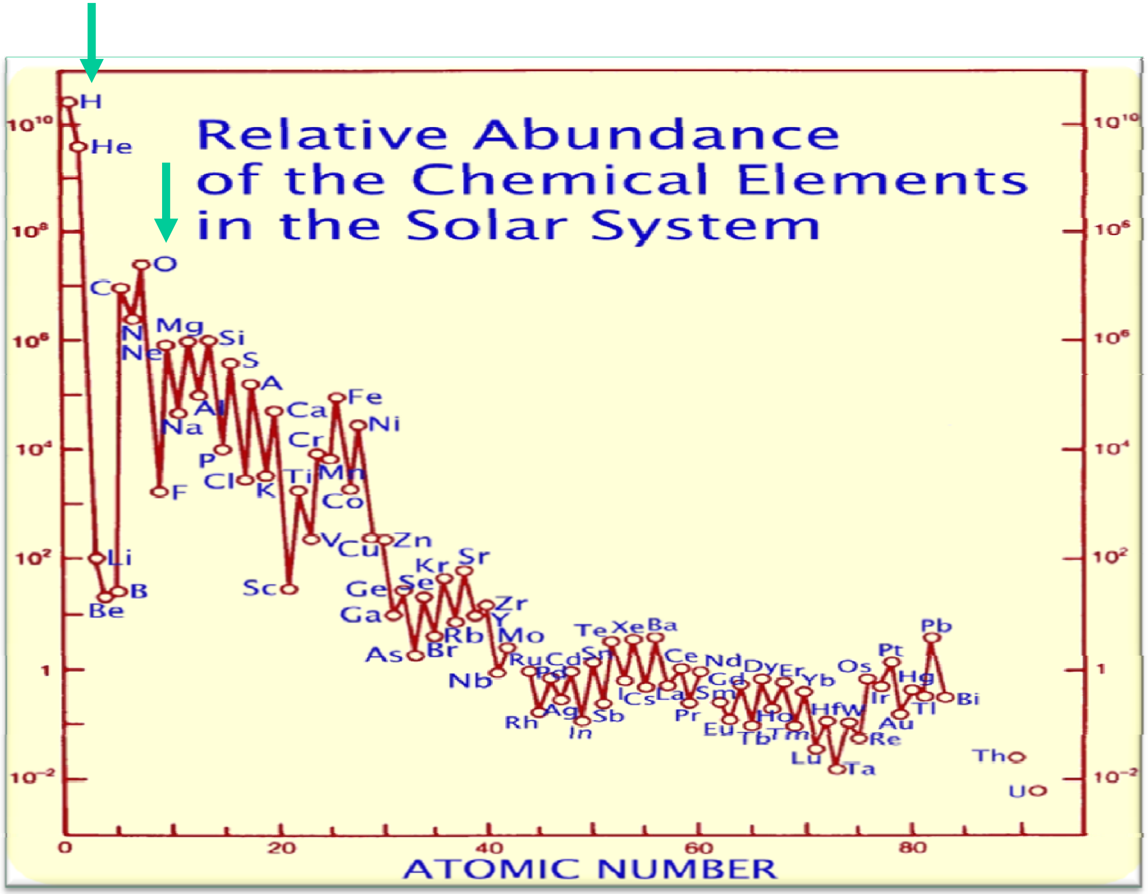

- H_2O consists of the first and third most abundant elements in the solar system, and plays an exceedingly important role in a wide range of geophysical, planetary, physical, chemical, and biological systems.

Phase Diagram of H_2O (before 2004)

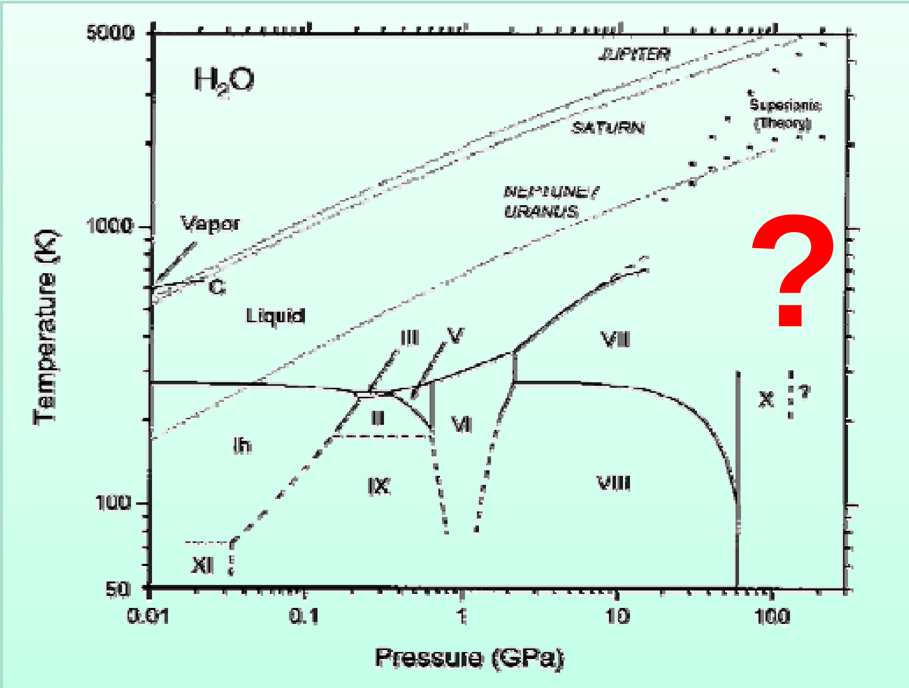

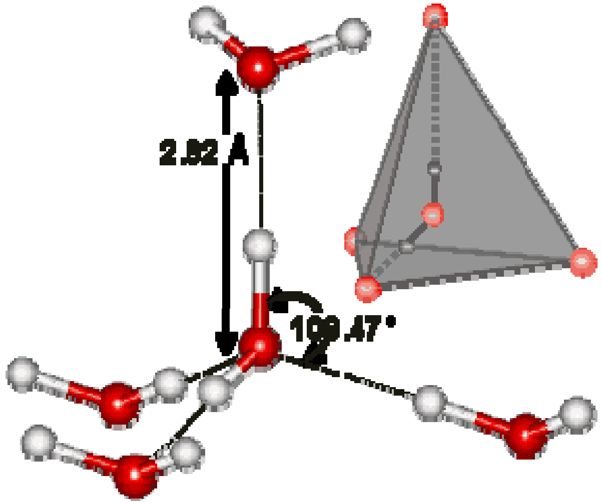

Structure of Ice Ih

After de Pater & Lissauer (2001)

- **There exist at least 15 phases including stable, metastable, crystalline, and amorphous phases of H_2O. All of these phases observed over modest P-T below 60 GPa conditions have structures closely dictated by the Pauling ice rules (Pauling, 1935). At higher pressures, symmetrization of the hydrogen-bonded network occurs, forming an ionic state, ice X.**

X-ray Raman Scattering (XRS)

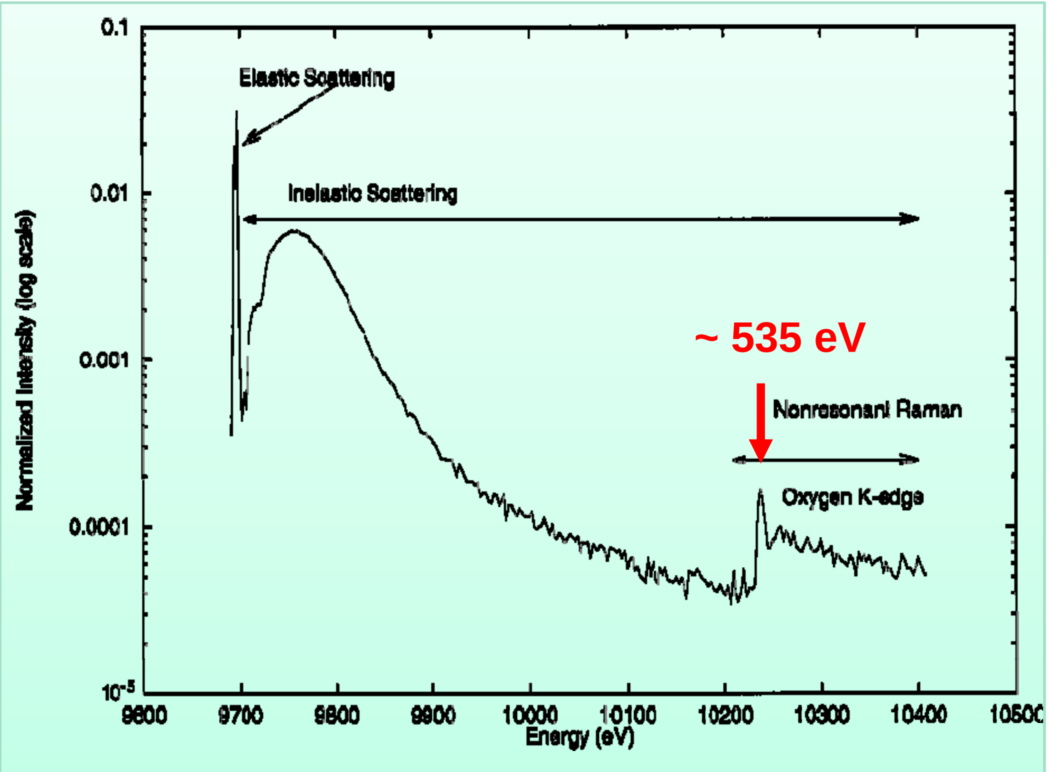

Bowron et al, Phys. Rev. B 62, R9223

- First observed by Das Gupta in the 1950's
- Clear connection to XAS was established theoretically by Mizuno and Ohmura and experimentally by Suzuki in 1967, with different strengths
- Synchrotron Radiation experiments by Tohji and Udagawa in 1987
- Established as a routine technique in the 1990's -- see work by Uwe Bergmann (Bergmann et al. Microc. 71 (2002) 221).
- High-pressure DAC applications in recent years

A powerful probe that provides detailed information on the local electronic bonding structure of light elements under high pressure

XAS versus XRS

- **The energy of the incident photon in XAS = The energy transfer in XRS**
  The momentum transfer q = photon polarization vector

XAS

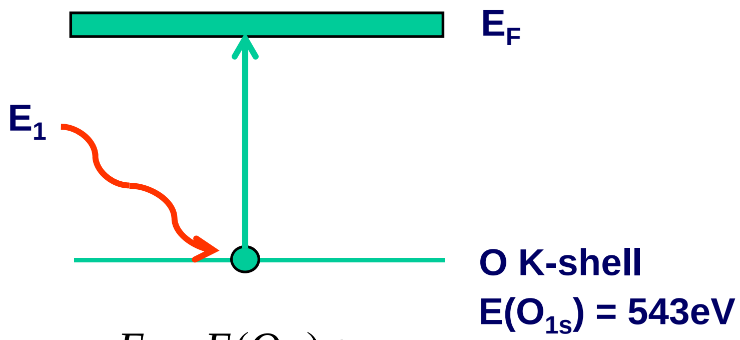

$$E_1 = E(O_{1s}) + e_k$$

XRS

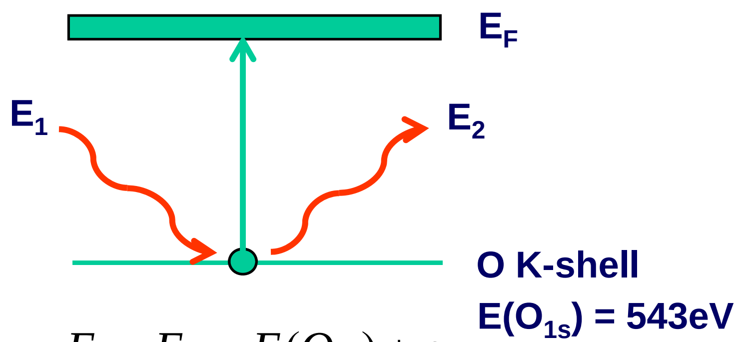

$$E_1 - E_2 = E(O_{1s}) + e_k$$

- **Limitations due to the use of soft x-rays for light elements:**
  Surface sensitivity
  Restricted sample environments
  e.g., incompatible with high pressure

- **Advantages of using hard x-rays :**
  Non-dipole regimes ($qr \geq 1$)
  True bulk sensitivity
  Flexible sample environments
  e.g., compatible with high pressure

(Yong Cai, NSLS-II Seminar, 11 April 2007)

XRS: Possible Applications

- **Various Systems**
  - Aqueous systems, organisms with high water content (vacuum non-compatible)
  - First and second row elements
  - Transition metal L edges and M-edges
- **High Pressure / Temperature**
  - Different forms of ice, supercritical water and aqueous solutions
  - Methane hydrates
  - N_2, O_2, CO, CO_2, NO, etc.
  - Hydrogen storage in nanotubes under pressure
  - Pressure-induced superconductivity (most light elements)
- **Notable High-Pressure Related Works:**
  - W.L. Mao *et al.*, "Bonding Changes in Compressed Superhard Graphite", SCIENCE **302**, 425 (2003)
  - Y. Meng *et al.*, "The Formation of sp^3 Bonding in Compressed BN", Nature Mat. **3**, 111 (2004)
  - Y.Q. Cai *et al.*, "Ordering of Hydrogen Bonds in High-Pressure Low-Temperature H_2O", Phys. Rev. Lett. **94**, 025502 (2005)
  - S.K. Lee *et al.*, "Probing of Bonding Changes in B_2O_3 Glasses at High Pressure with Inelastic Xray Scattering", Nature Mat. 4, 851 (2005).
  - W.L. Mao *et al.*, "X-ray-induced Dissociation of H_2O and Formation of an O_2-H_2 Alloy at High Pressure", SCIENCE **314**, 636 (2006).

Proton Disordered to Ordered Transition

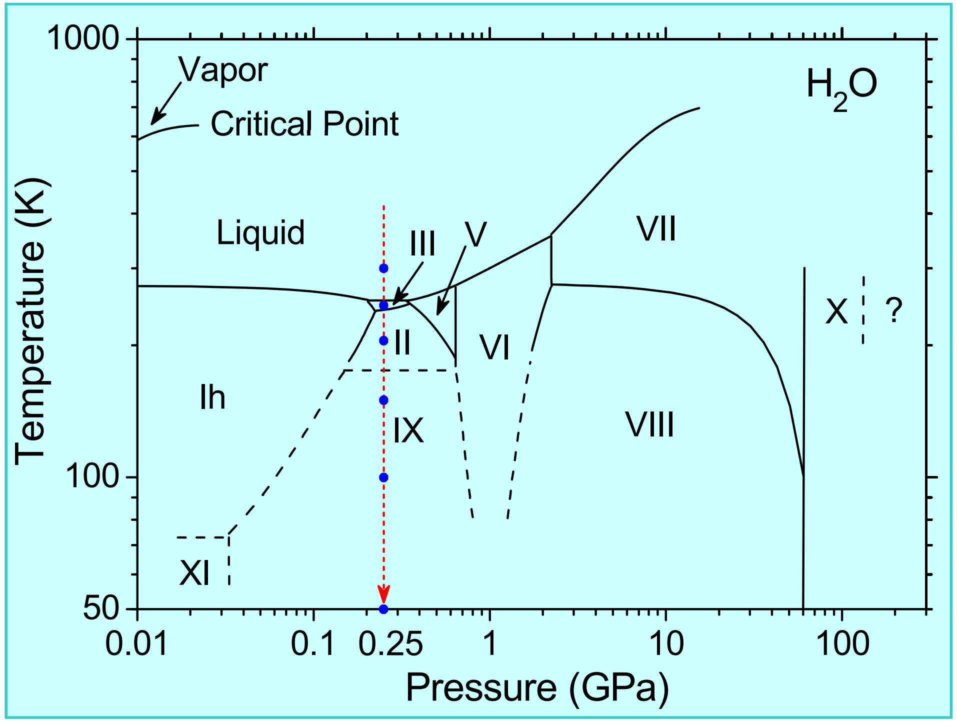

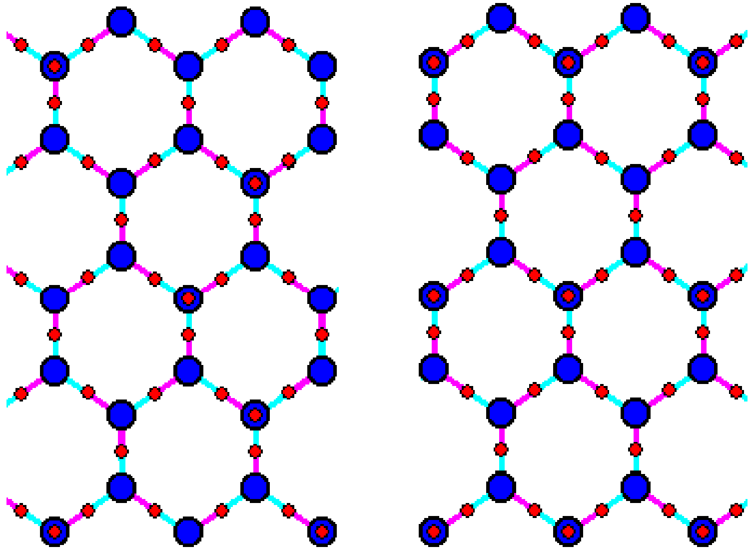

Disordered **Ordered**

(after S. Dutch, University of Wisconsin)

- **Proton disordered to ordered phase transitions:**
  ice III – ice IX (two O sites)
  ice VI – ice VIII (one O sites)

Ice polymorph	Crystal structure	Proton Network
Ice III / ice VI	Tetragonal	Disordered
Ice II	Rhombohedral	Ordered
Ice IX / ice VIII	Tetragonal	Ordered

National Synchrotron Radiation Research Center

SPring-8

(Yong Cai, NSLS-II Seminar, 11 April 2007)

Effect of Proton-Ordering in H_2O

- High resolution (300meV) allows fine details of the edge structure to be resolved !

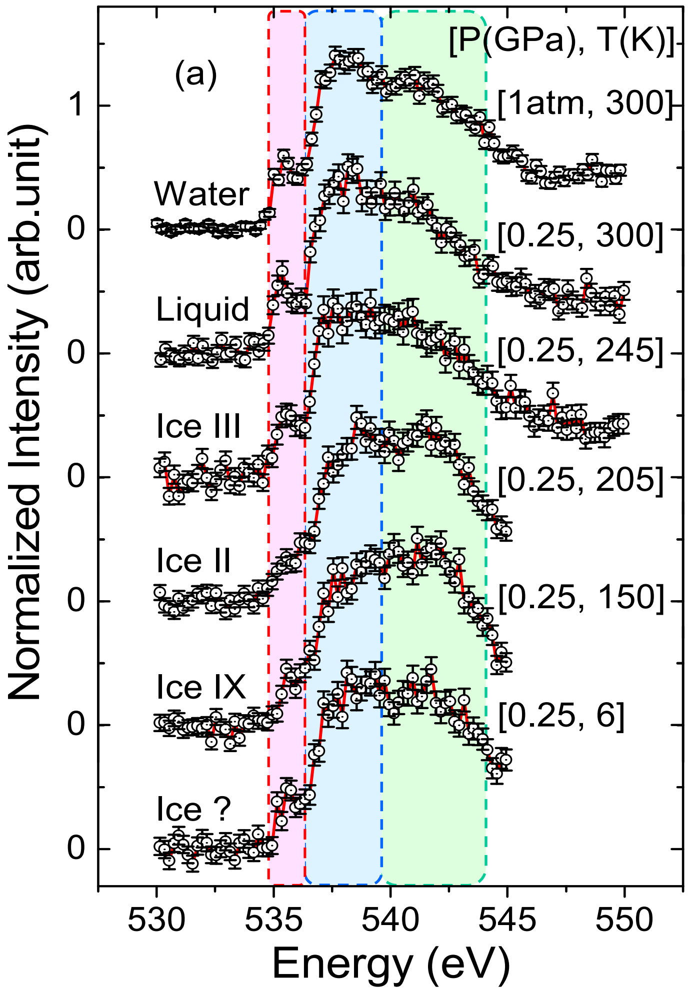

Pre-, Main-, Post-edge

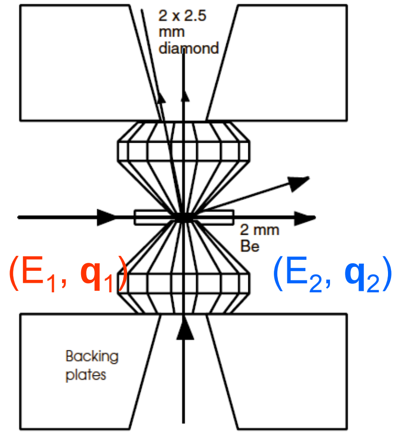

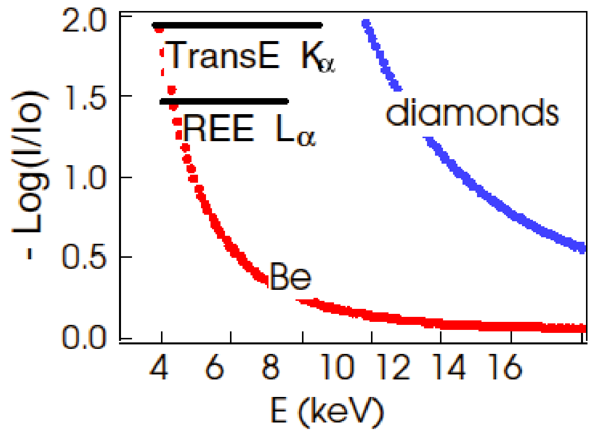

Scattering thru Be: Less absorption, larger angular range!

Ice polymorph	Crystal structure	Proton Network
Ice III	Tetragonal	Disordered (~75%)
Ice II	Rhombohedral	Ordered (100%)
Ice IX	Tetragonal	Ordered (~92%)

The decrease of the pre-edge intensity is a key signature of proton ordering in the H_2O frame work!

(Cai et al, Phys. Rev. Lett. 94, 025502)

National Synchrotron Radiation Research Center

SPring-8

(Yong Cai, NSLS-II Seminar, 11 April 2007)

A New LT Phase ?

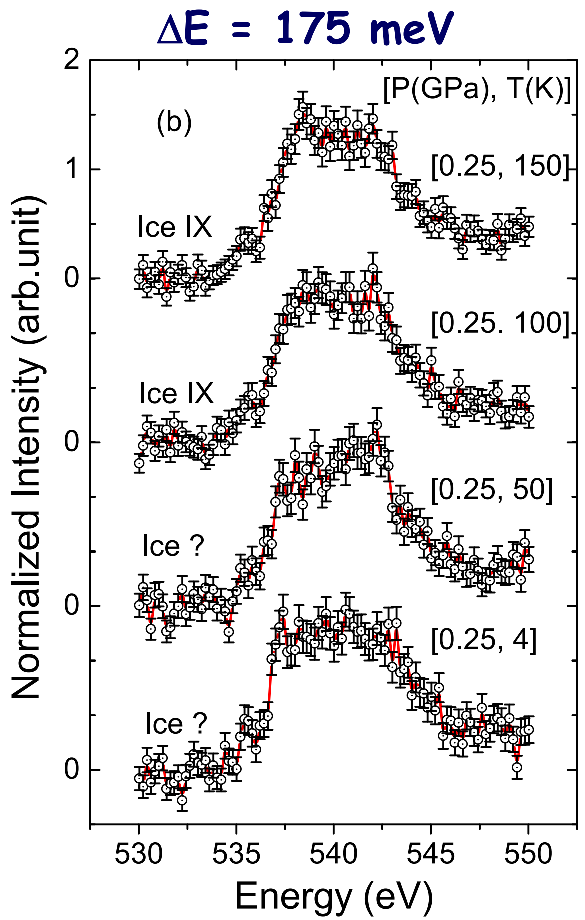

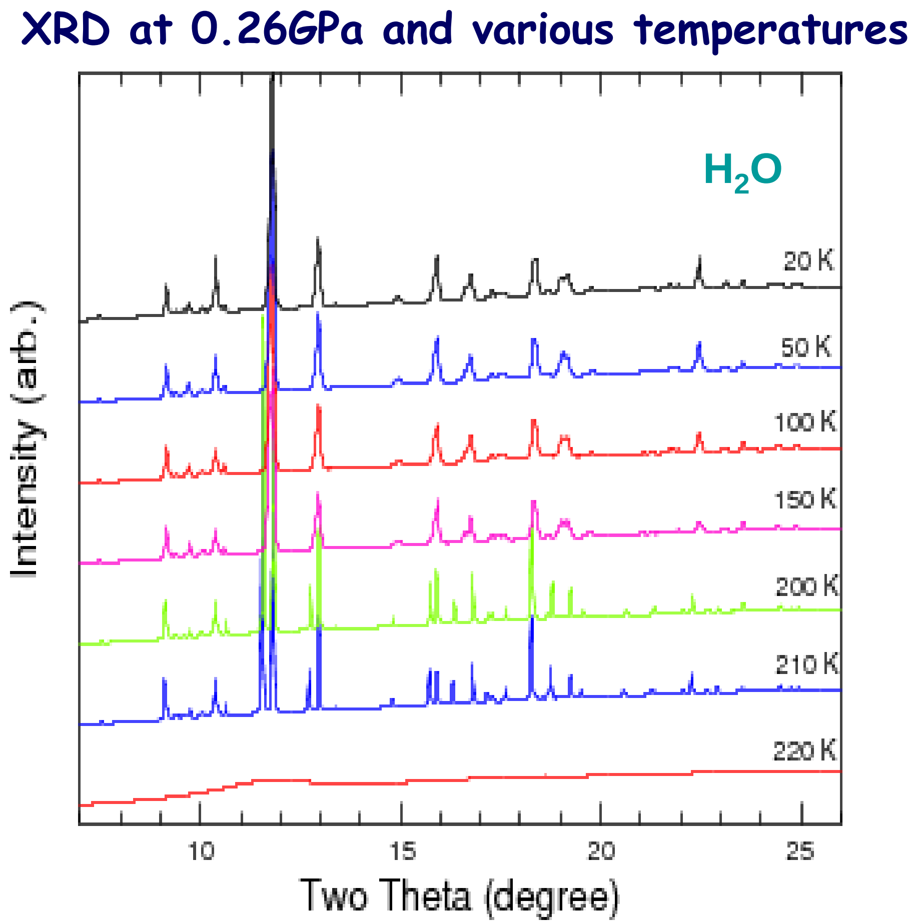

XRS: is a sensitive probe to local bonding variations
XRD: provides information on long-range structural variations

(Cai et al, unpublished)

X-ray-induced Dissociation of H_2O

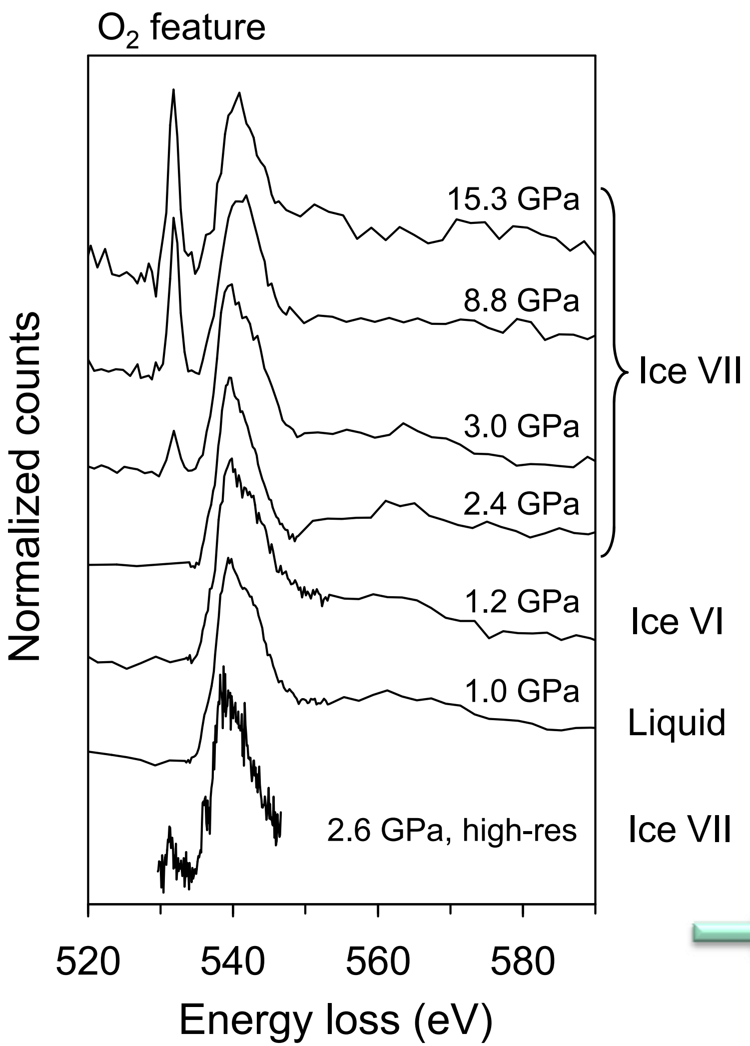

Before and after X-radiation

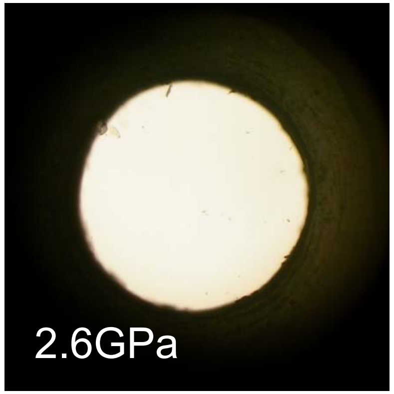

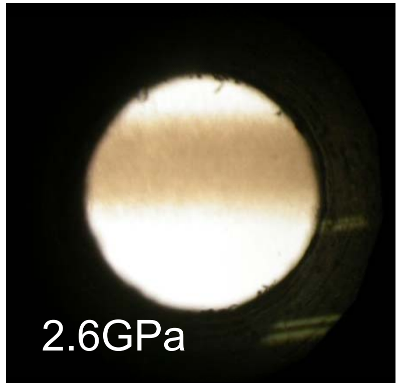

At pressure above 2.5 GPa, H_2O cleaves under prolong x-radiation and forms a new alloy of H_2 and O_2 molecules that does not follow Pauling's ice rules!

⟹ **New way to study H_2 and O_2 interaction**

(W.L. Mao et al, Science 314, 636)

Synergy for HP Sciences

- **An excellent example of HP research that illustrates the necessity of using a multitude of experimental techniques for proper characterization of the system (A scenario of Elephant and the Blind Men) .**

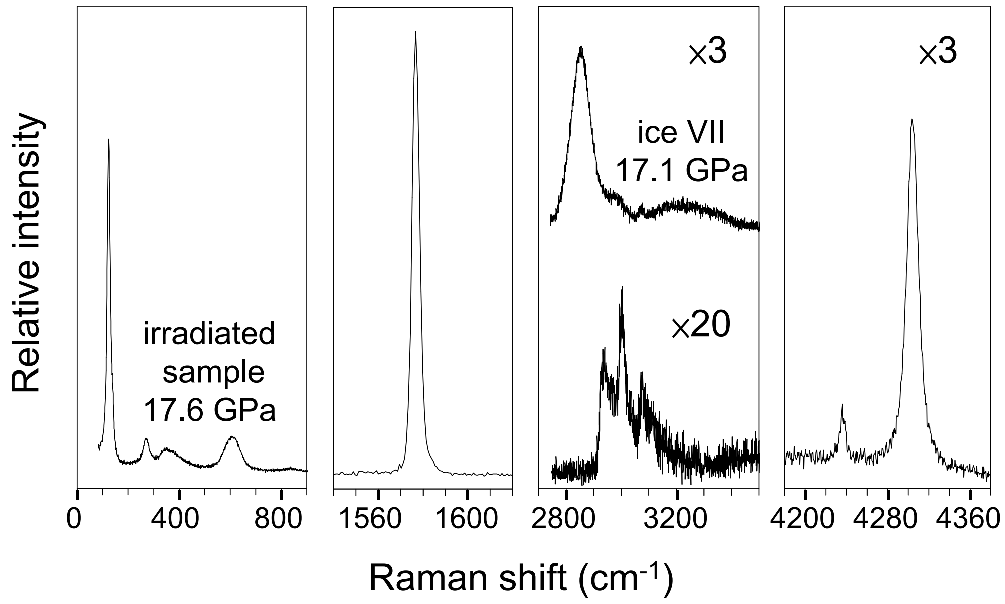

Laser Raman Spectroscopy

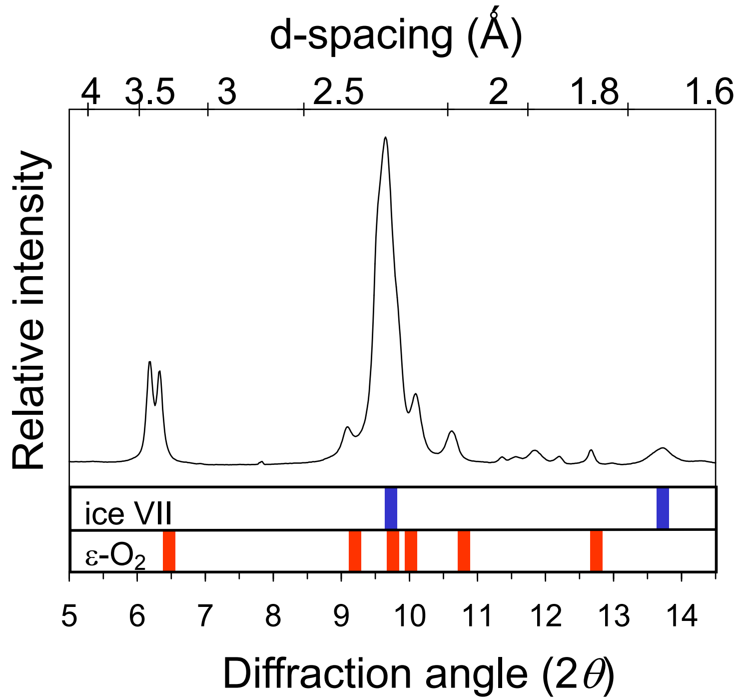

X-ray Diffraction

(W.L. Mao et al, Science 314, 636)

Outline

- Brief Review of IXS by Electronic Excitations
  - Theory and Experiment (BL12XU Setup)
- **Performance and Selected Results**
  - Element-Specific Applications (XRS/XES/FPY-XAS)

    XRS: High pressure phases of H_2O, liquid & solid He, SiO_2, Ba_8Si_{46} ...

    XES/XAS: P/T-induced charge instability in TmTe, Prussian Blue ...
  - **Low-Energy Charge Dynamics in (ω,q) Space (NIXS/RIXS)**

    NIXS: Graphite, MgB_2, Py-SO, $CaMnO_3$, NiO ...

    RIXS at the K-edge of TM: NiO, Sr_2CuO_3, La_2CuO_4/La_2NiO_4 ...
- Possible Further Developments and Outlook
  - Possible further developments
  - Outlook with the Taiwan Photon Source

NIXS of Charge Dynamics: Key Aspects

$$S(\mathbf{q},\omega) = -\frac{\hbar q^2}{4\pi^2 e^2 n}\cdot \mathrm{Im}\,\varepsilon^{-1}(\mathbf{q},\omega) = -\frac{1}{\pi n}\cdot \mathrm{Im}\,\chi(\mathbf{q},\omega)$$

- **Fluctuation-Dissipation Theorem links $S(q,\omega)$ to $\varepsilon(q,\omega)$, the latter defines all physical responses of the target system to external field: Insight into the excitations of the N-particle many-body system and their interplay with the electronic structure:**

$$\mathbf{D}_{Internal} = \varepsilon \mathbf{E}_{external} = (\varepsilon_1 + i\varepsilon_2)\mathbf{E}_{external}$$

- **Generally, $\varepsilon(q,\omega)$ is a complex function of momentum and energy**
  - The real part represents features of collective excitations (e.g., plasmons)
  - The imaginary part describes single-particle excitation (e.g., interband transitions).
  - For core excitations, the real part and the imaginary part are well decoupled ($\varepsilon_1 \sim 1$, $\varepsilon_2 \sim \mu$), while they are strongly coupled for valence excitations

NIXS v's Optical & EELS Studies

- Compared to optical studies (q=0), the q-dependent information provides full knowledge of the charge dynamics and a stringent test of theory
- IXS is almost free of multiple scattering (cf. EELS), even at high q, providing a clean way to study the charge dynamics at high q, where short-range correlation effects showing interesting and new physics can be expected
- Cross section is proportional to q^2, in contrast to q^{-4} in the case of EELS
- At sufficiently high q, non-dipole transitions become possible, allowing additional excitation channels to be explored
- One derives ε (q, ω) by using the f-sum rule:

$$\int \mathrm{Im}\,\varepsilon^{-1}(\mathbf{q},\omega)\omega d\omega = -2\pi^2 e^2 n/m$$

and the Kramer-Kronig transformation:

$$\varepsilon_1(\mathbf{q},\omega) = 1 + \frac{2}{\pi} P\int_0^\infty \frac{\omega' \varepsilon_2(\mathbf{q},\omega')}{(\omega')^2 - \omega^2} d\omega'$$

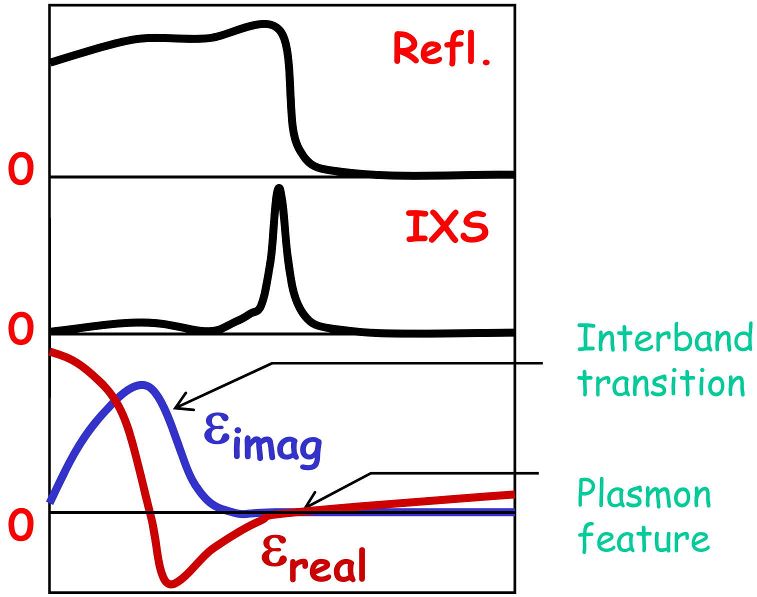

⟹ Practical application of NIXS to study ε (q, ω) has just started !

Graphite

- Similar crystallographic and electronic structure to C-based novel materials C_{60} or nanotubes
- Various types of properties such as superconductivity, H storage, or super hard form, induced by intercalation, nano-structuring, or applying pressure

Crystal structure

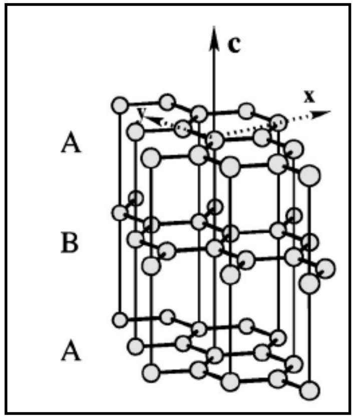

Brillouin zone

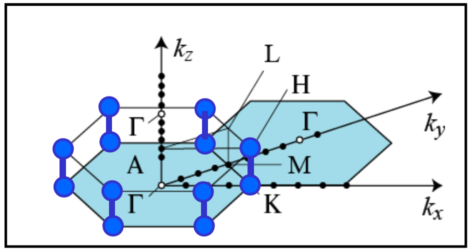

Gapless

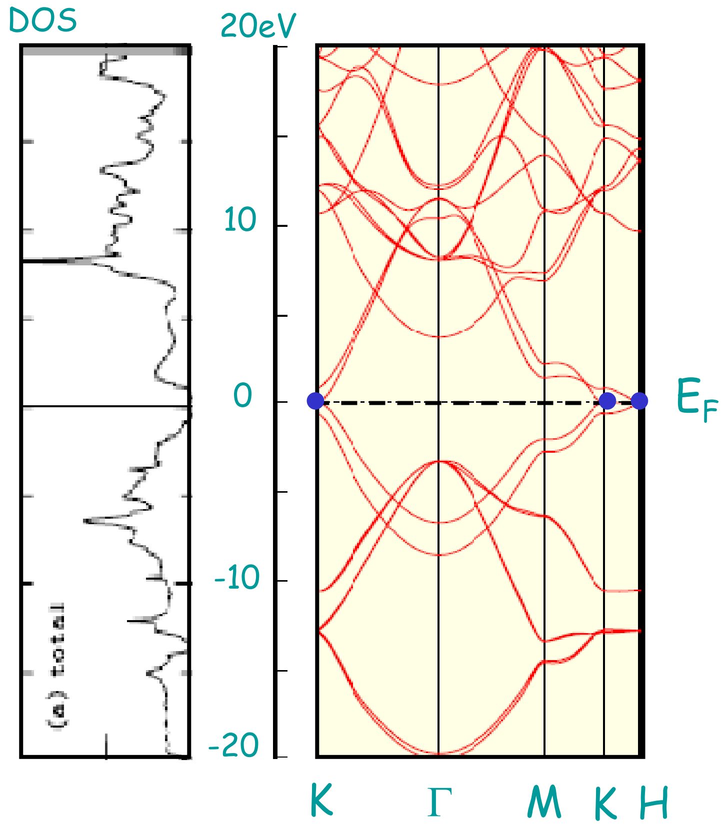

An important fact is that graphite is semi metallic. However, there are few reports that have observed semi-metallic electronic structure.

Graphite

IXS spectra:

Collective mode and single-particle mode are mixed.

KK Transform.

Dielectric function

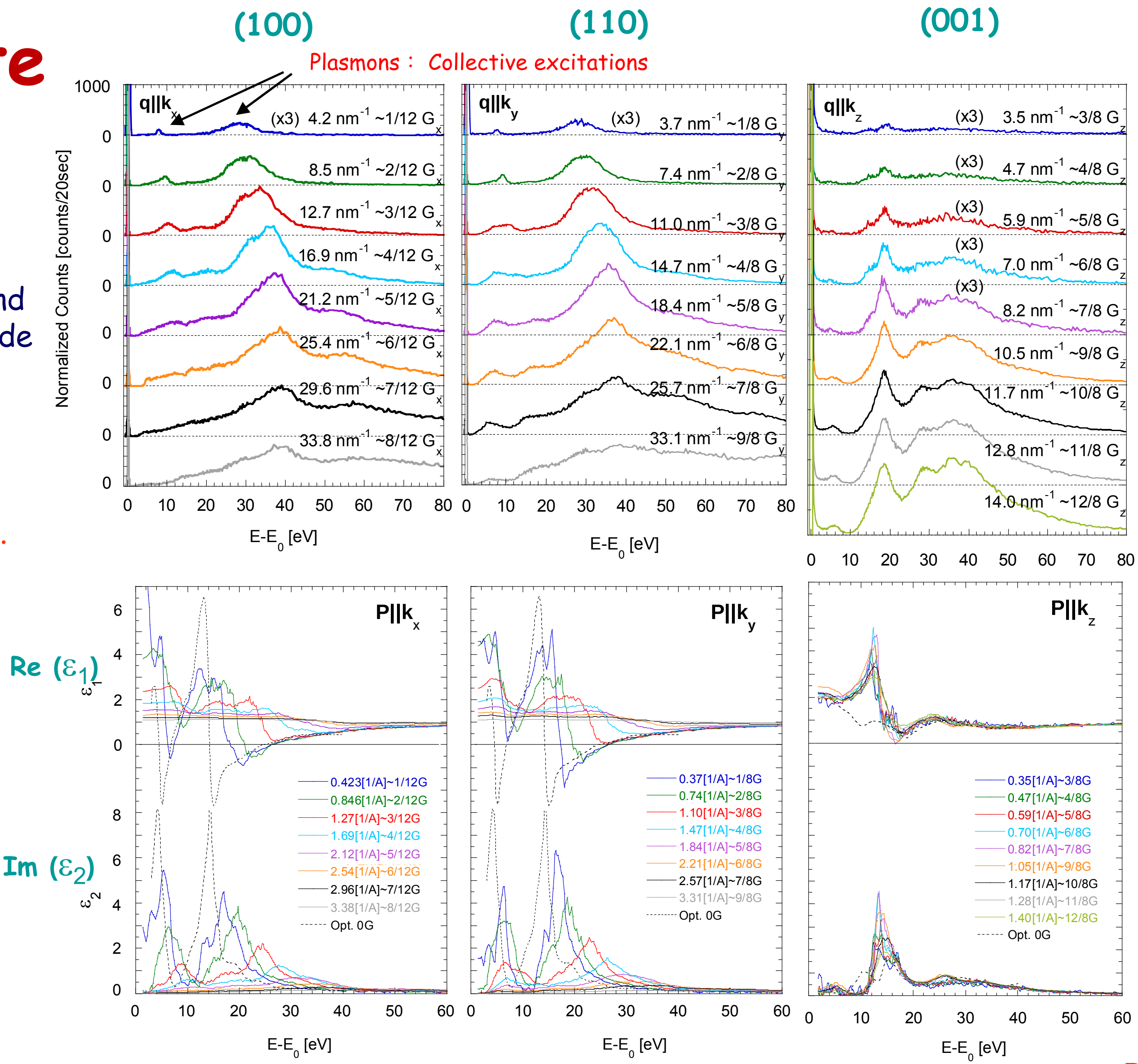

(Hiraoka et al. Phys. Rev. B 72, 075103)

Graphite

*Optical data: EXP. Klucker et al. Phys. Status Solidi B **65** 703 (1974)
THEO: Marinopolous et al. Phys. Rev. B **69** 245419 (2004)

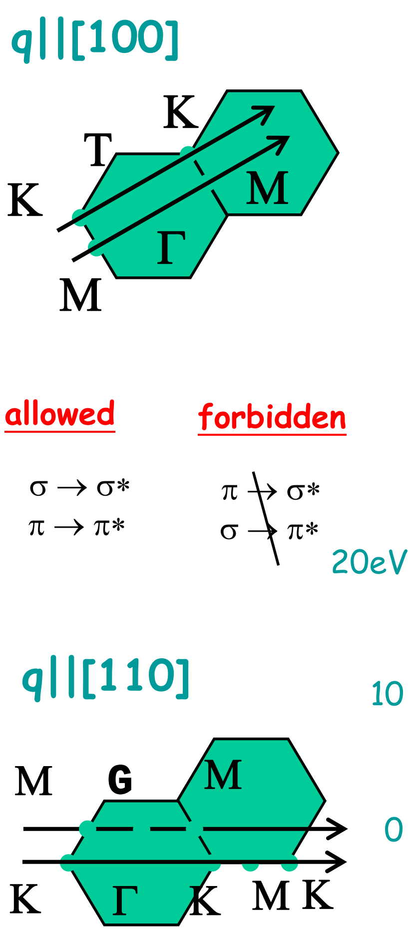

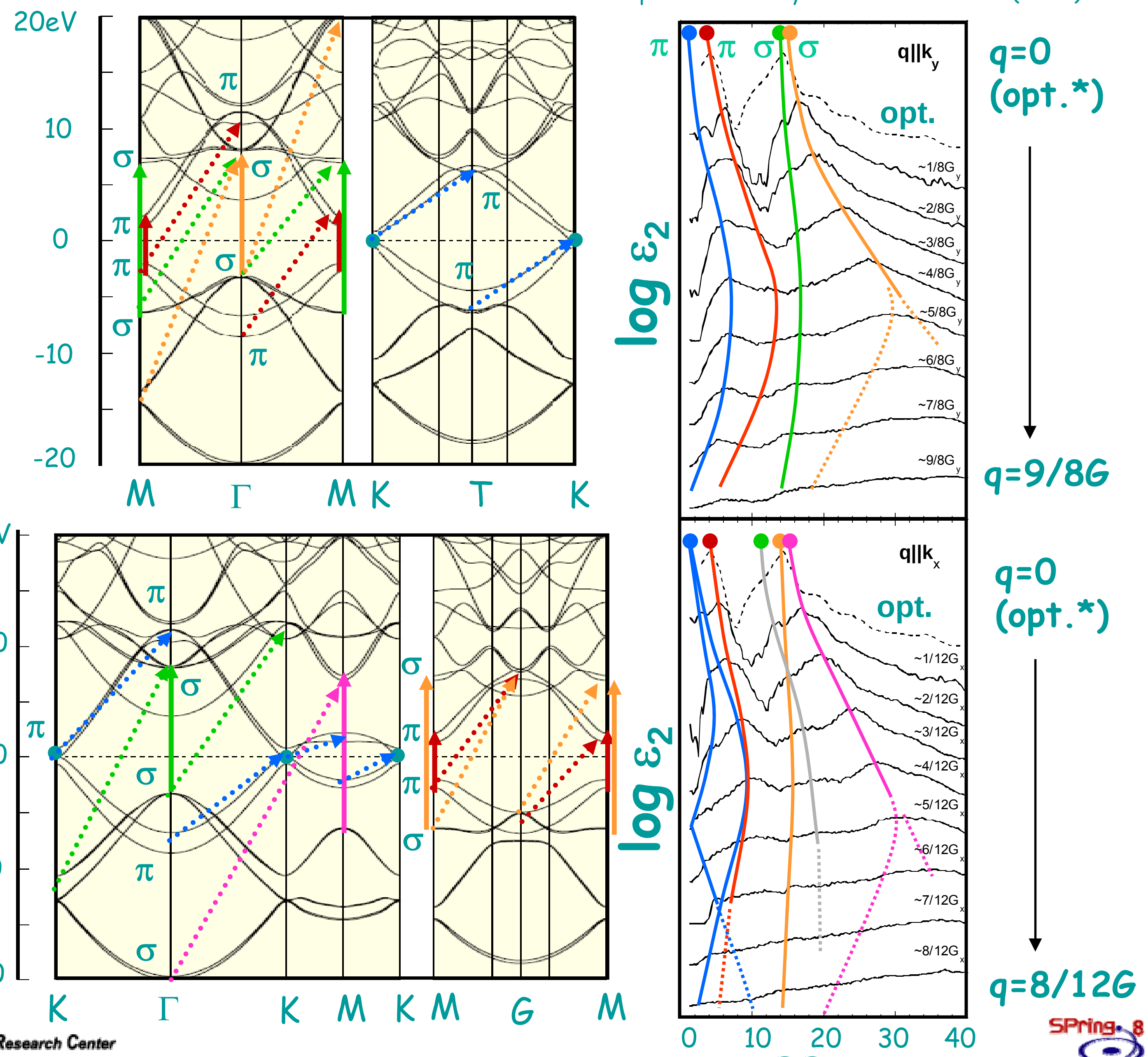

National Synchrotron Radiation Research Center

IXS clearly observes semi-metallic features in graphite

SPring-8

(Yong Cai, NSLS-II Seminar, 11 April 2007)

Superconductivity of MgB_2

- **Superconductivity (T_c=39K) is dominated by strong e-p coupling between the B sub-lattice (the E_{2g} optical phonons) and the 2D boron σ bands**

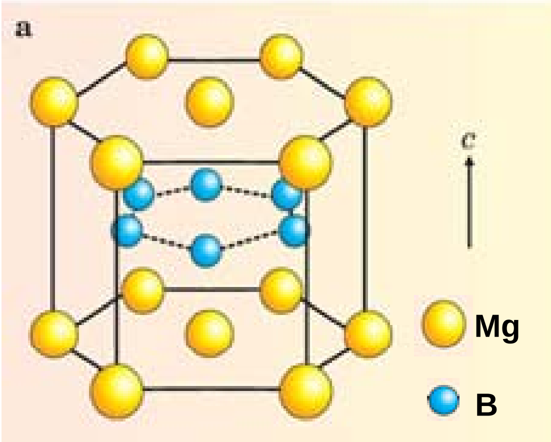

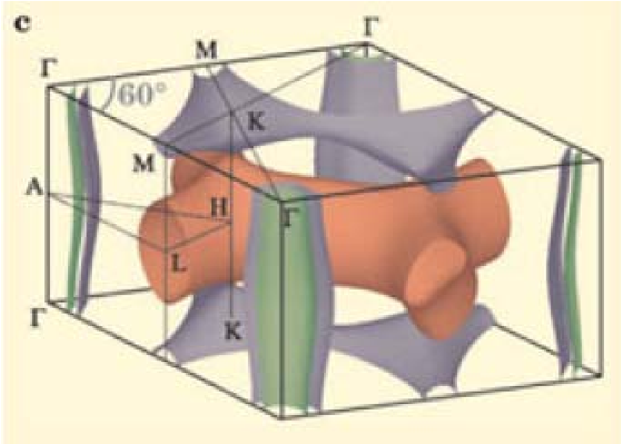

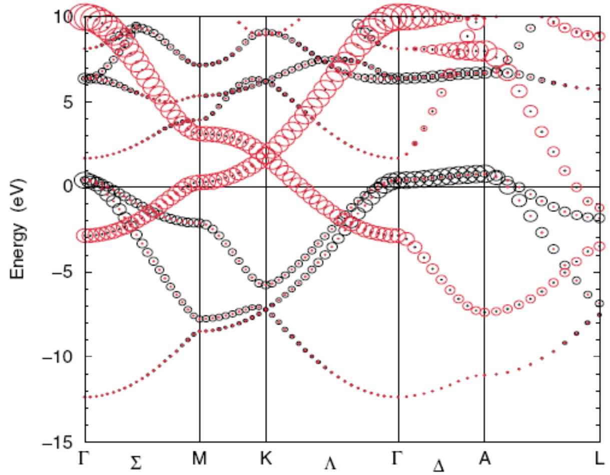

Strong charge inhomogeneity | ***Kortus et al, Phys. Rew. Lett. 86, 4656*** | **O B π-bands** **O B σ-bands**

- **The Realization of a Demon?**

Demon = distinct electron motion (D. Pines, 1956), formed in the presence of two distinct types of carriers in the system (the heavy B 2D σ holes and the light 3D π electrons in MgB_2). The light carriers could screen the Coulomb repulsion of the heavy carriers effectively, thereby reducing the plasmon frequency of the heavy carriers, leading to the so-called acoustic plasmon that follows generally: $\omega_a = v_a q$, where v_a ~ the Fermi velocity of the heavy carriers.

Dynamical Response of MgB_2

(W. Ku et al, Phys. Rev. Lett. 88, 057001)

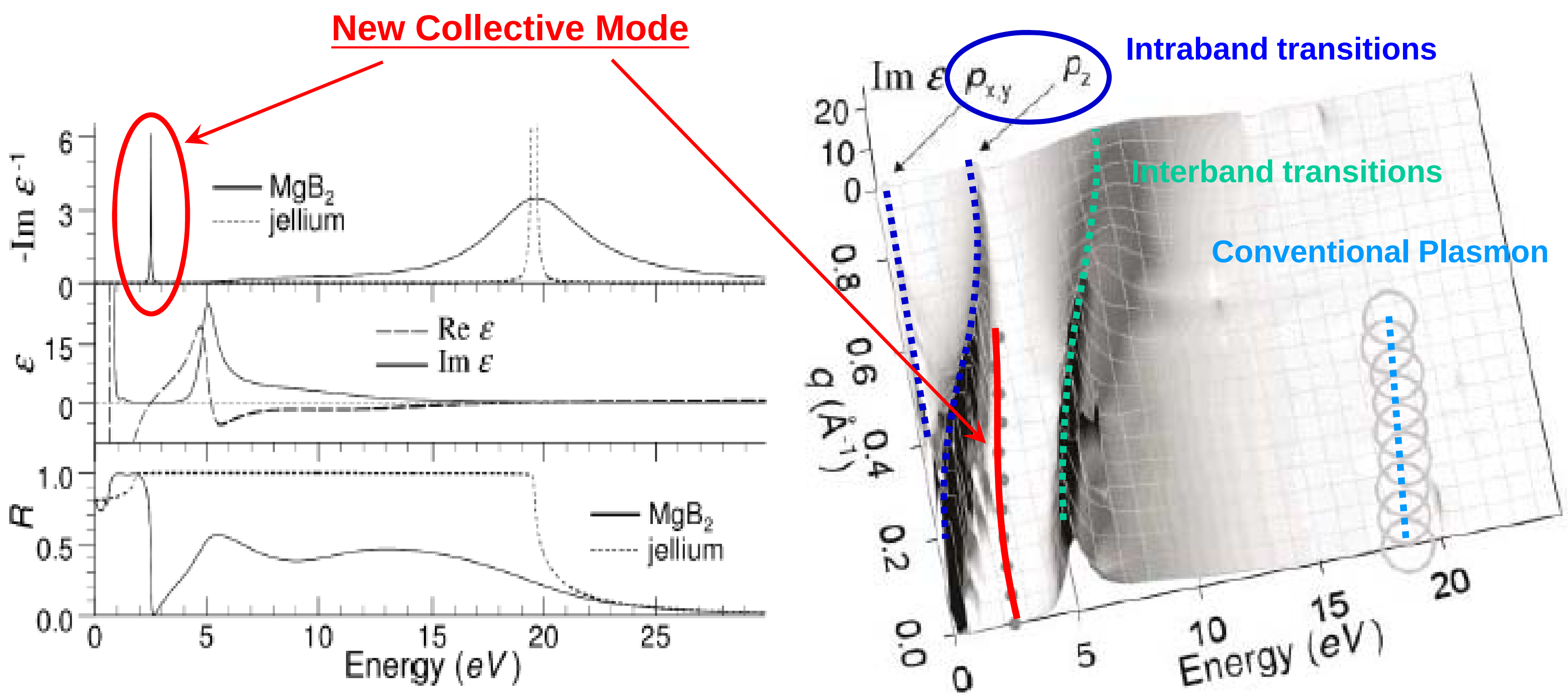

- At low q, crystal-local field effects (CLFE) are negligible, the new collective mode disappears into particle-hole continuum by Landau damping as q increases

Charge Dynamics in (ω,q) Space: MgB_2

q//c-axis [001]   ΔE = 250 meV

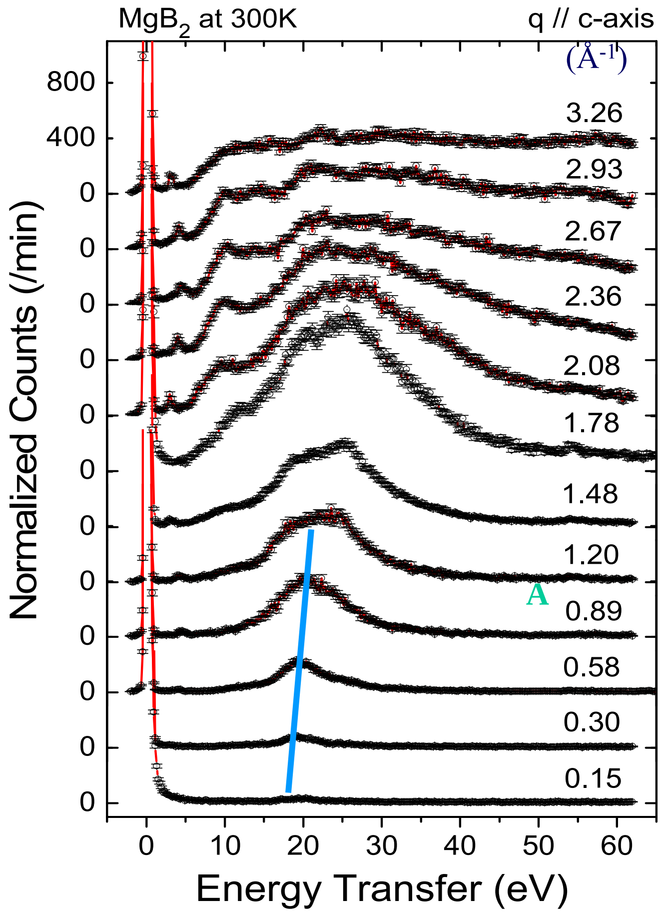

Δq = 0.06 Å^{-1}

q//a-axis [100] ΔE = 65 meV

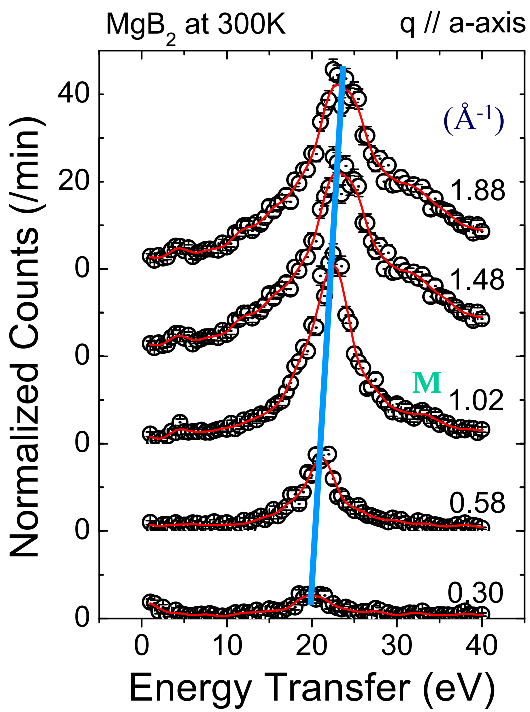

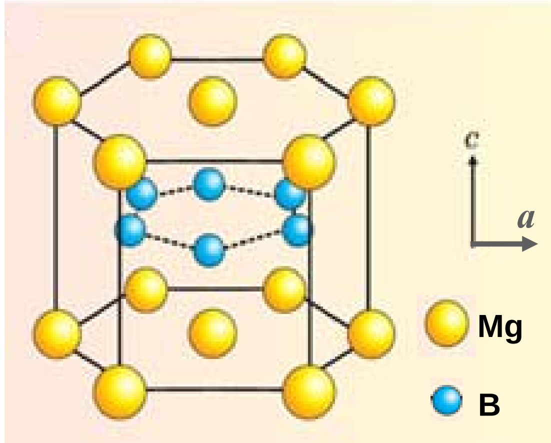

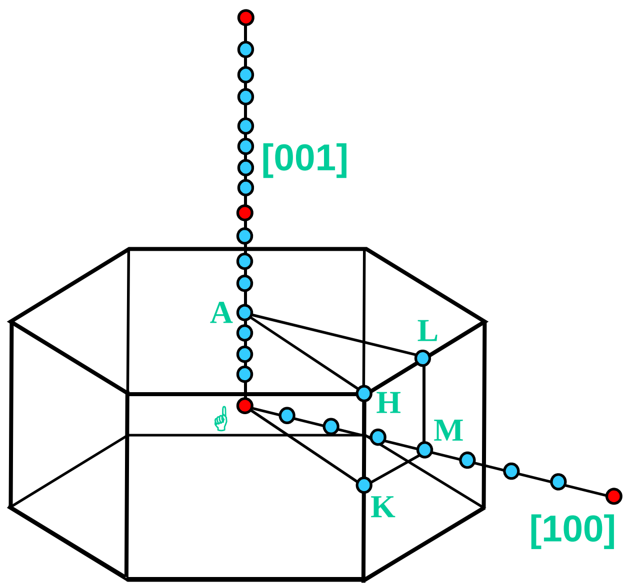

Bulk plasmon of conduction electrons

Low-Energy Charge Excitations: q//c*-axis

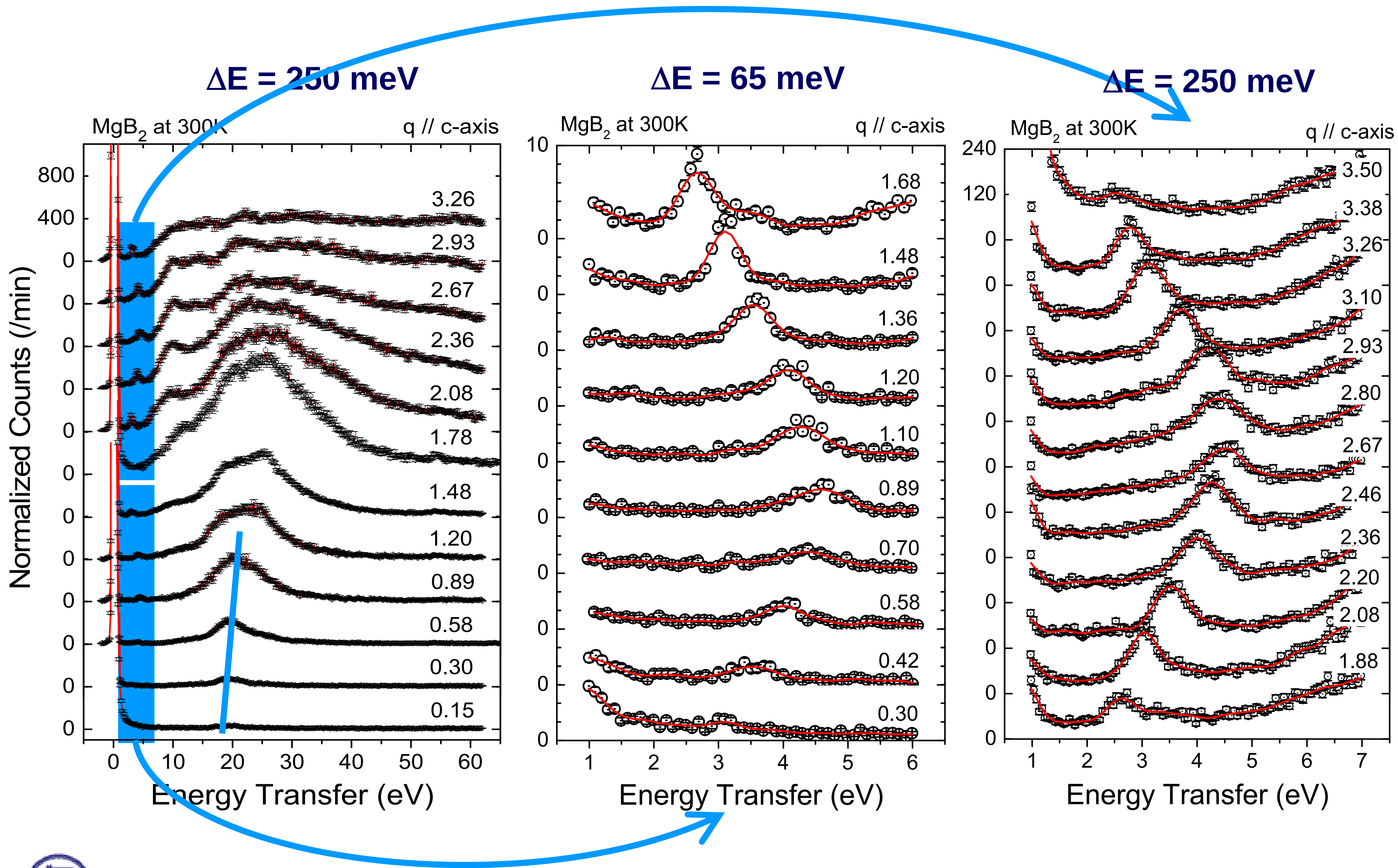

(Cai et al, Phys. Rev. Lett. 97, 176402)

Periodic Dispersion: q//c*-axis

First ever periodic collective charge excitation observed in a metallic system !

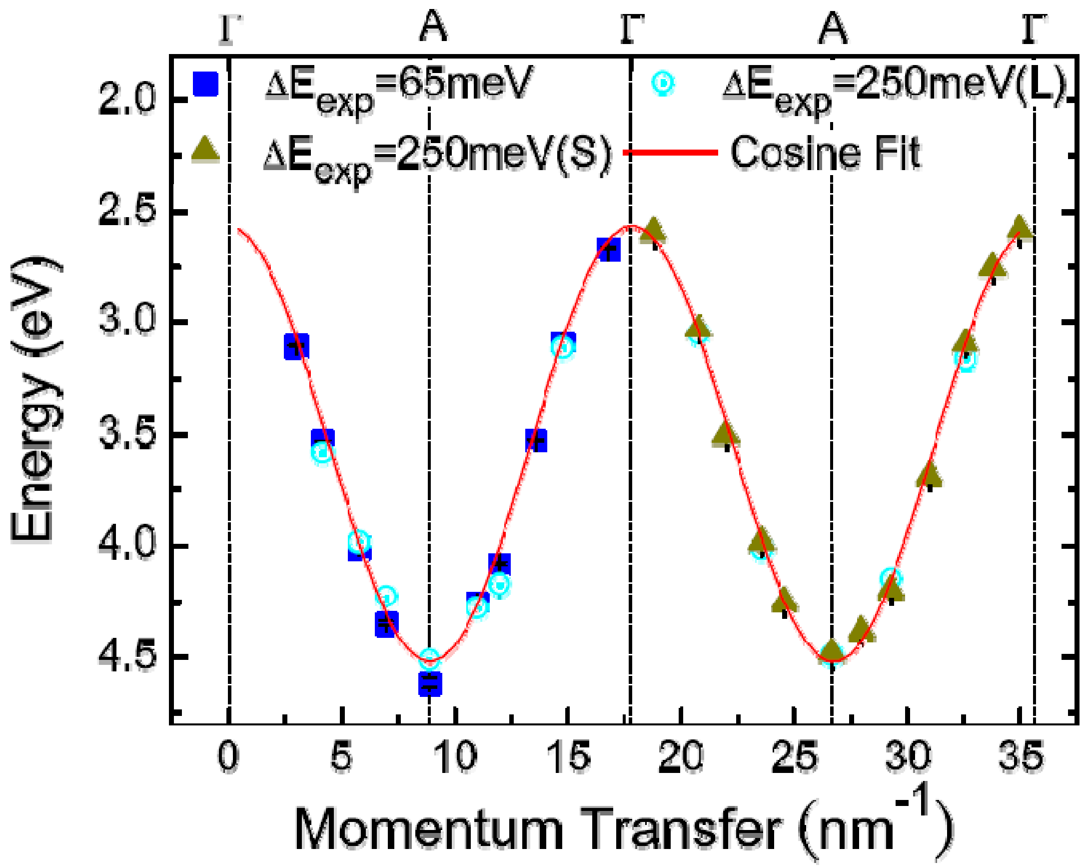

- Empirical energy dispersion follows entirely a cosine function :

$$\omega = \omega_0 - 2\gamma \cos(qc)$$

ω_0 = 3.55 eV
γ = 0.49 eV
c = 3.52 Å

Periodicity of Dielectric Function

$$\varepsilon_{\vec{G},\vec{G}'}\left(\vec{q}-\vec{G}_q;\omega\right)=\varepsilon_{\vec{G},\vec{G}'}\left(\vec{k};\omega\right)$$

Periodicity of the Dielectric Response?

The density-response matrix can be expressed in terms of the ***inverse*** of the dielectric matrix as

$$\chi_{\vec{G},\vec{G}'}\left(\vec{q}-\vec{G}_q;\omega\right)=v^{-1}\left(\vec{q}-\vec{G}_q+\vec{G}\right)\left(\left[\varepsilon\left(\vec{q}-\vec{G}_q;\omega\right)\right]^{-1}_{\vec{G},\vec{G}'}-\delta_{\vec{G},\vec{G}'}\right)$$

For the latter, we have derived the exact result,

$$\left[\varepsilon\left(\vec{q}-\vec{G}_q;\omega\right)\right]^{-1}_{\vec{G}_q,\vec{G}_q}=\frac{1}{\varepsilon_{\vec{G}_q\vec{G}_q}\left(\vec{q}-\vec{G}_q;\omega\right)}$$

$$+F\left(\vec{q},\vec{q}-\vec{G}_q;\omega\right)\left[\varepsilon\left(\vec{q}-\vec{G}_q,\omega\right)\right]^{-1}_{\vec{G}=\vec{0},\vec{G}=\vec{0}}$$

for q's in BZ's higher than the first one.

MgB_2: Strong CLFE at Large q !

- **Matrix Response to Include CLFE**

$$\left[\varepsilon(\mathbf{q}-\mathbf{G_q},\omega)\right]^{-1}_{\mathbf{G_q},\mathbf{G_q}} = \frac{1}{\varepsilon_{\mathbf{G_q},\mathbf{G_q}}(\mathbf{q}-\mathbf{G_q},\omega)} + F(\mathbf{q},\mathbf{q}-\mathbf{G_q};\omega)\left[\varepsilon(\mathbf{q}-\mathbf{G_q},\omega)\right]^{-1}_{0,0}$$

- ***F* Function is Material-Dependent**

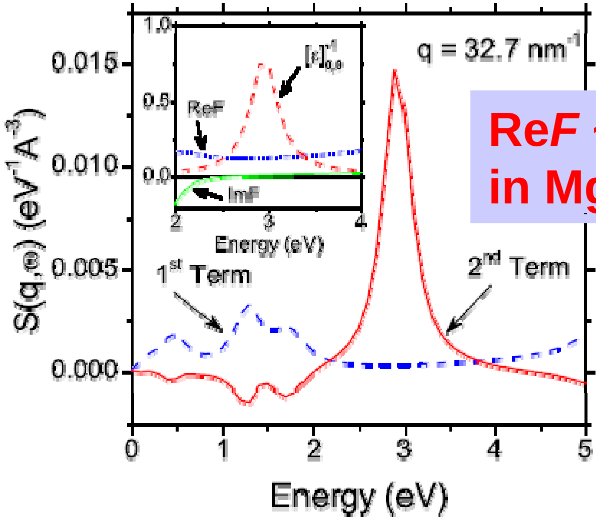

Re*F* ~ 60 times larger in MgB_2 than Al, Si !

S(q,ω)

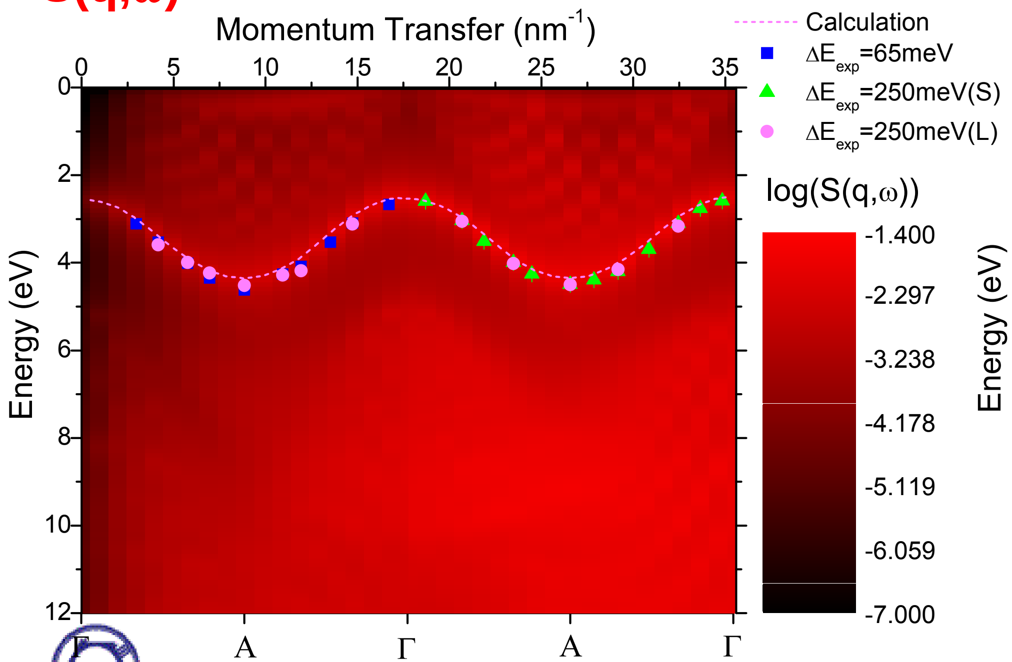

Imε(q,ω)

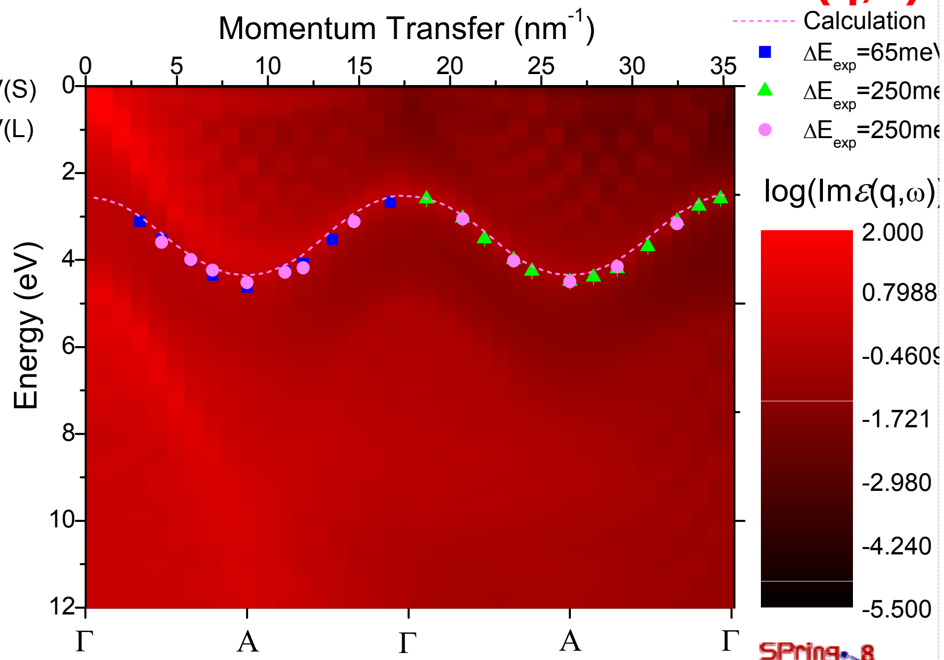

National Synchrotron Radiation Research Center

(Cai et al, Phys. Rev. Lett. 97, 176402)

SPring-8

(Yong Cai, NSLS-II Seminar, 11 April 2007)

Outline

- Brief Review of IXS by Electronic Excitations
  - Theory and Experiment (BL12XU Setup)
- Performance and Selected Results
  - Element-Specific Applications (XRS/XES/FPY-XAS)

    XRS: High pressure phases of H_2O, liquid & solid He, SiO_2, Ba_8Si_{46} ...

    XES/XAS: P/T-induced charge instability in TmTe, Prussian Blue ...
  - Low-Energy Charge Dynamics in (ω, q) Space (NIXS/RIXS)

    NIXS: Graphite, MgB_2, Py-SO, $CaMnO_3$, NiO ...

    RIXS at the K-edge of TM: NiO, Sr_2CuO_3, La_2CuO_4/La_2NiO_4 ...
- **Possible Further Developments and Outlook**
  - **Possible further developments**
  - **Outlook with the Taiwan Photon Source**

Future Plan 1

IXS under high pressure at low temperature (already started)

- Dynamic variation of temperature and pressure
- Laser Raman spectroscopy to ensure phases of samples.

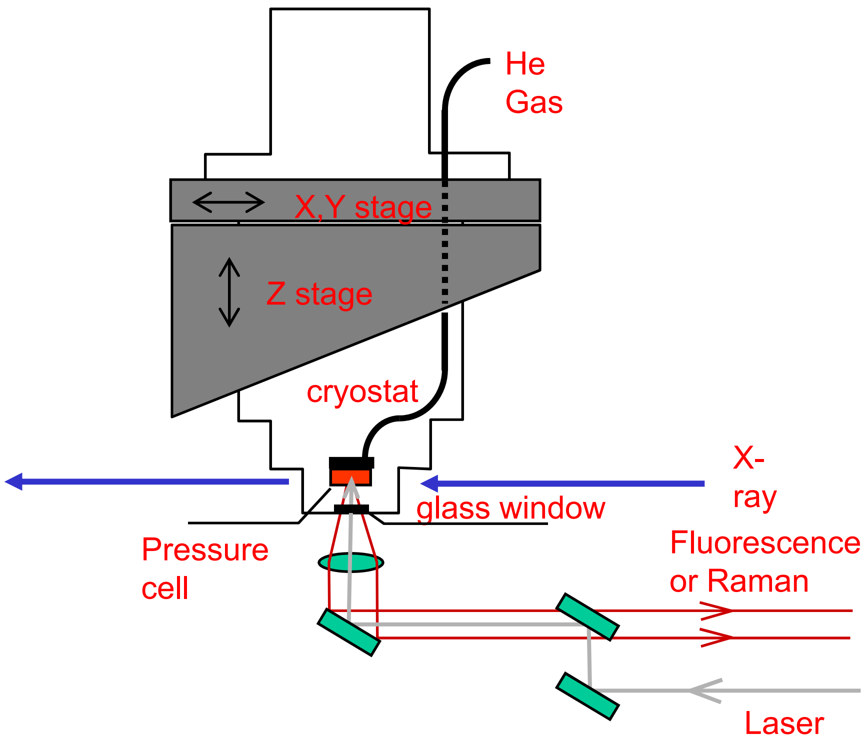

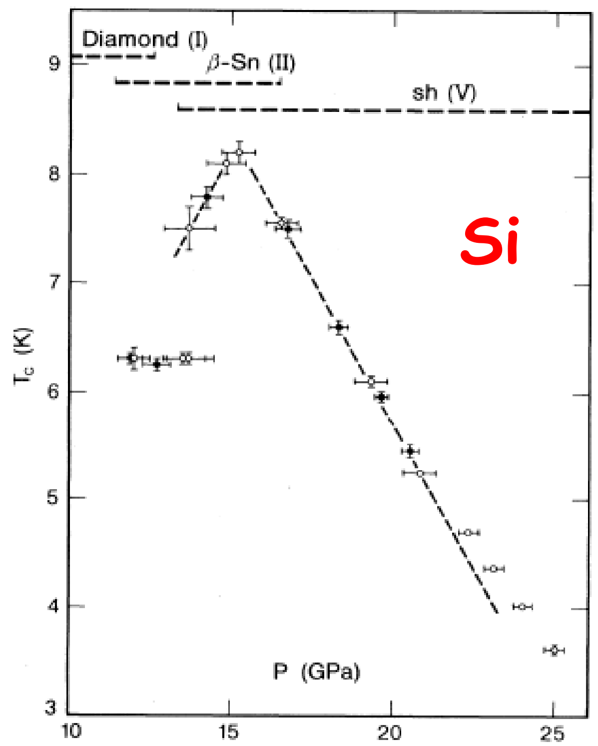

Chang et al. Phys. Rev. Lett. 54 2375 (1985)

Future Plan 2

IXS using 20 keV photons

- High penetration power for XRS of compounds of heavy elements
- Increased flexibility for high pressure experiments (e.g., no-Be gaskets)
- RIXS on 4d, 5f compounds (E_B ~ 20 keV)

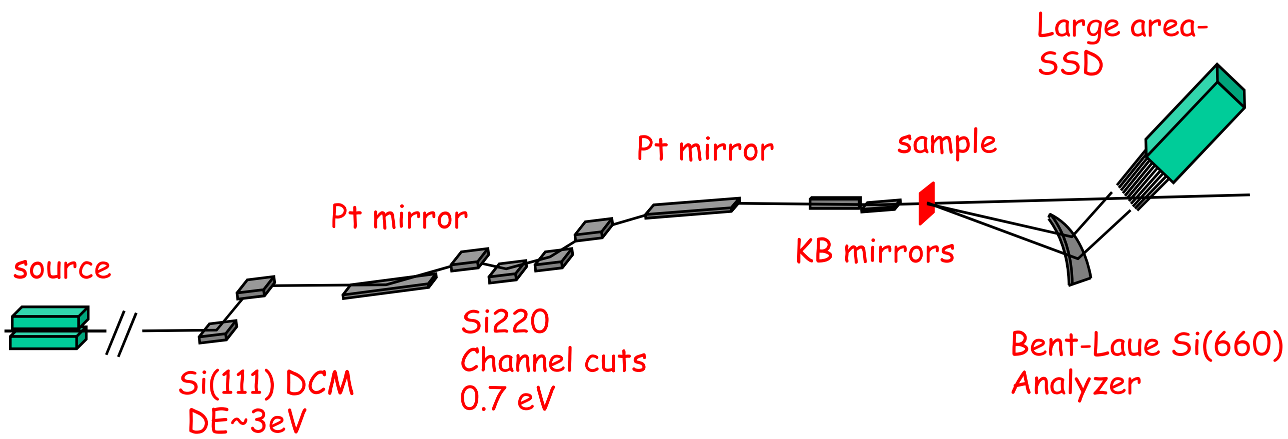

- Total energy resolution : ~ 1 eV
- Flux: 5 x 10^{12} photons/sec/eV
- Beam size : 20 x 20 μm^2
- Energy transfer range: ~ 1 keV
- q-range : 10 ~ 200 nm^{-1}
- Count-rate : ???

New 3-GeV Taiwan Photon Source (TPS)

1. Instrumentation Building
2. Utility Building I
3. Utility Building II
4. TPS Utility Building
5. TLS Storage Ring
6. Research Building
7. Administration Building
8. TPS Storage & Booster Ri
9. International Activity Cent
10. Medical Imaging Lab

TPS Parameters – Not the Final

TPS	Non-achromatic 24p18K1	Achromatic 24p18L1
Energy (GeV)	3.0	
Beam current (mA)	400	
Circumference (m)	518.4	
Nat. emittance ε_x(nm-rad)	1.7 (ε_{xeff} = 2.17 LS center)	5.8
Cell / symmetry / structure	24 / 6 / DBA	
β_x / β_y / η_x (m) LS middle	10.59 / 9.39 / 0.11	12.9 / 9.79 / 0.0
RF frequency (MHz)	499.654	
RF voltage (MV)	3.5	
Harmonic number	864	
SR loss/turn, dipole (MeV)	0.98733	
Straights	11.72m*6+7m*18	
Betatron tune ν_x /ν_y	26.22 / 12.28	26.24 / 12.28

Brilliance Comparison with Other Sources

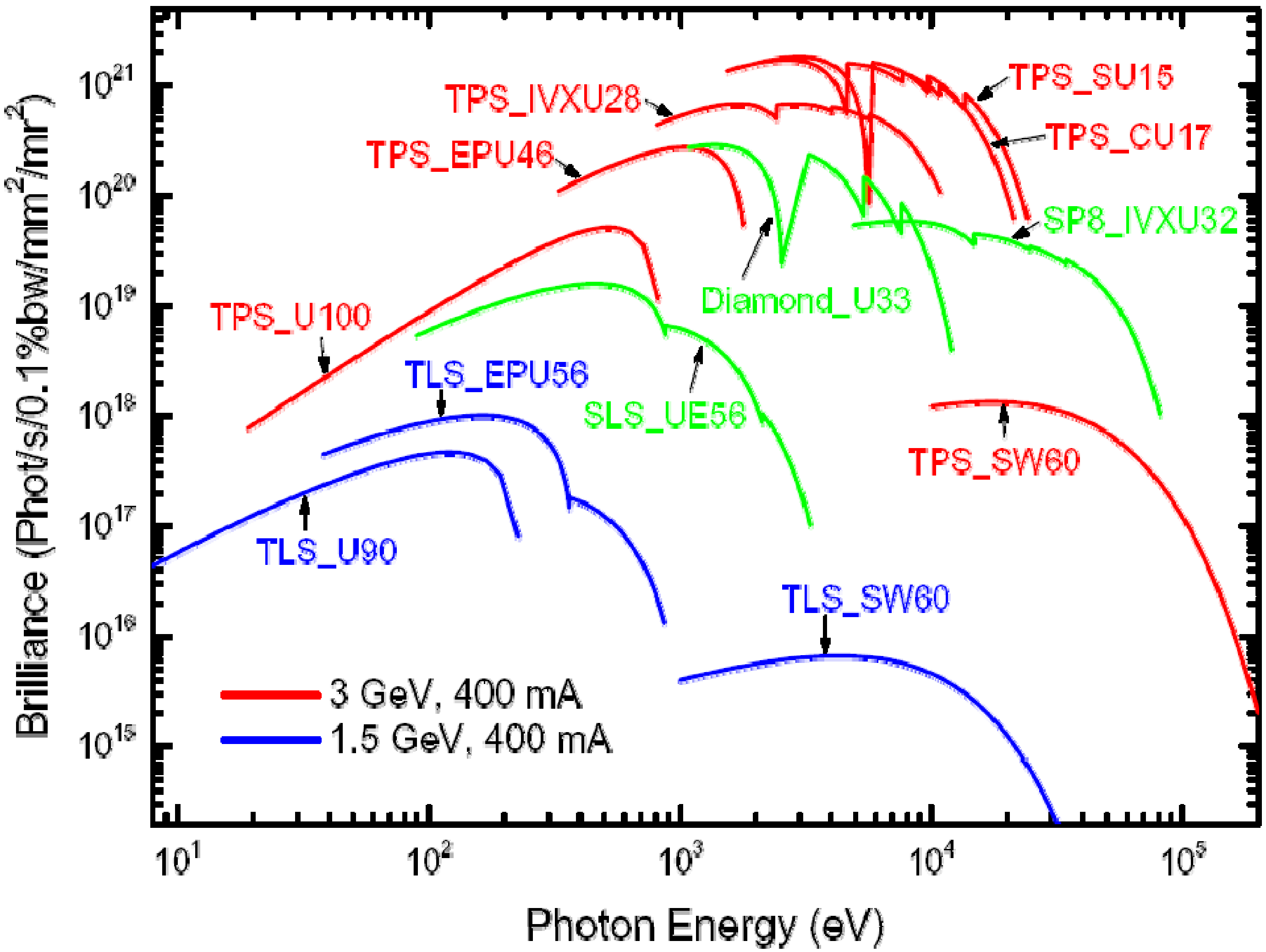

	SU15
Photon energy (keV)	2.5-25
Current (mA)	400
λ(mm)	15
N_{period}	133
By (Bx) (T)	1.5
K_{max}	2.1
L (m)	2
Gap (mm)	5.6
Peak Power density (kW/mr²)	170
Total power (kW)	23.5
Type	SC

National Synchrotron Radiation Research Center

SPring-8

(Yong Cai, NSLS-II Seminar, 11 April 2007)

Summary

- Versatile, state-of-the-art IXS facilities at 3rd generation synchrotrons provides a powerful probe of the charge dynamics of a wide variety of systems, including those under extreme pressure and temperature.
- The improved energy and momentum resolution and wide scan range have allowed experimental dielectric functions to be studied with unprecedented details.
- IXS experiments are flux limited. An ideal instrument should therefore provide the flexibility that allows maximum available flux within the appropriate energy band width for the problem to be attacked.
- New 3rd generation medium energy rings such as the NSLS-II and the TPS provide new opportunities and challenges.

Acknowledgements

- NSRRC
  - Nozomu HIRAOKA
  - Hirofumi ISHII
  - Ignace JARRIGE (now with JAEA)
  - Paul CHOW (now at HP-CAT, APS)
  - Cheng-Chi CHEN: Mechanical Engineering
  - Shen-Yaw PERNG: Analyzer Development
  - Duan-Jen WANG: Analyzer Development
  - Chien-Te CHEN: Project Director
- Key Collaborators
  - Chi-Chang KAO, BNL, USA
  - Eric SHIRLEY, NIST, USA
  - John S. TSE, NRC, Canada
  - Wei KU, Phys., BNL, USA
  - Adolfo G. EGUILUZ, UT, USA
  - Dave MAO, GL-CIW, USA
  - Donglai FENG, U. Fudan, China
  - Changyoung Kim, Yonsei U., Korea
  - Alfred BARON, RIKEN/JASRI, Japan
  - Shik SHIN, RIKEN, Japan
  - Ahbay SHUKLA, U. P&M. Curie, France
  - Jean-Pascal RUEFF, Soleil, France
- Funding
  - NSC and NSRRC

Thank You!